Table

Sequences of Quantitative RT-PCR primers

Probe	Primer 1	Primer 2
MCP-1	5'-actgaagccagctctctcttcctc-3'	5'-ttccttcttggggtcagcacagac-3'
IL-6	5'-caatgctctcctaacagataag-3'	5'-aggcataacgcactaggt-3'
IL-1β	5'-caagcaatacccaaagaaga-3'	5'-gaaacagtccagcccatac-3'
CRP	5'-cagcttctctcggacttttg-3'	5'-aggtgttcagtggcttctttg-3'
TNFα	5'-aggtcaatctgcccaagt-3'	5'-gggctgggtagagaatg-3'
catalase	5'-aggtgttgaacgaggagga-3'	5'-ctcagcgttgtacttgtcca-3'
GST	5'-tgccaagatcaaggaacaaa-3'	5'-ccacatggtagaggagttcaa-3'
MnSOD	5'-ggtcgcttacagattgct-3'	5'-ctcccagttgattacattcc-3'
GAPDH	5'- accacagtccatgccatcac -3'	5'- tccaccaccctgttgctgta -3'

Cardiovascular Research (2008) 79, 287–293
doi:10.1093/cvr/cvn110

LOX-1 deletion decreases collagen accumulation in atherosclerotic plaque in low-density lipoprotein receptor knockout mice fed a high-cholesterol diet

Changping Hu[1,2†], Abhijit Dandapat[1†], Liuqin Sun[1,3], Jiawei Chen[1], Muhammad R. Marwali[1], Francesco Romeo[4], Tatsuya Sawamura[5], and Jawahar L. Mehta[1*]

[1]*Department of Internal Medicine, Central Arkansas Veterans Healthcare System and University of Arkansas for Medical Sciences, 4301 West Markham Street, Slot 532, Little Rock, AR 72205, USA;* [2]*Department of Pharmacology, School of Pharmaceutical Sciences, Central South University, Changsha, China;* [3]*Department of Ophthalmology, Heping Hospital, Changzhi Medical College, Changzhi, China;* [4]*Department of Cardiology, University of Rome 'Tor Vergata', Rome, Italy; and* [5]*Department of Vascular Physiology, National Cardiovascular Center Research Institute, Suita, Osaka, Japan*

Received 13 January 2008; revised 22 April 2008; accepted 25 April 2008; online publish-ahead-of-print 3 May 2008

Time for primary review: 21 days

KEYWORDS
Atherosclerosis;
LOX-1;
Extracellular matrix;
Matrix metalloproteinases;
NADPH oxidase

Aims Collagen, as a component of the extracellular matrix, has been linked to atherosclerotic plaque formation and stability. Activation of LOX-1, a lectin-like oxidized low-density lipoprotein (LDL) receptor-1, exerts a significant role in collagen formation. We examine the hypothesis that LOX-1 deletion may inhibit collagen accumulation in atherosclerotic arteries in LDL receptor (LDLR) knockout (KO) mice.

Methods and results We generated LOX-1 KO and LOX-1/LDLR double KO mice on a C57BL/6 (wild-type mice) background and fed a 4% cholesterol/10% cocoa butter diet for 18 weeks. Vessel wall collagen accumulation was increased in association with atherogenesis in the LDLR KO mice ($P < 0.01$ vs. wild-type mice), but much less so in the double KO mice ($P < 0.01$ vs. LDLR KO mice). Collagen accumulation data were corroborated with pro-collagen I measurements. Expression/activity of osteopontin, fibronectin, and matrix metalloproteinases (MMP-2 and MMP-9) was also increased in the LDLR KO mice ($P < 0.01$ vs. wild-type mice), but not in the mice with LOX-1 deletion ($P < 0.01$ vs. LDLR KO mice). The expression of NADPH oxidase ($p47^{phox}$, $p22^{phox}$, $gp91^{phox}$, and Nox-4 subunits) and nitrotyrosine was increased in the LDLR KO mice ($P < 0.01$ vs. wild-type mice) and not in mice with LOX-1 deletion ($P < 0.01$ vs. LDLR KO mice). Phosphorylation of Akt-1 and endothelial nitric oxide synthase and expression of haem-oxygenase-1 were found to be reduced in the LDLR KO mice ($P < 0.01$ vs. wild-type mice), but not in the mice with LOX-1 deletion ($P < 0.01$ vs. LDLR KO mice).

Conclusion LOX-1 deletion reduces enhanced collagen deposition and MMP expression in atherosclerotic regions via inhibition of pro-oxidant signals.

1. Introduction

Atherogenesis involves lipid accumulation, especially oxidized low-density lipoproteins (ox-LDLs),[1] endothelial injury,[2] chronic inflammation[3] and oxidative stress.[4] Besides the accumulation of lipids, atherosclerotic regions are characterized by the presence of fibrous elements in different layers of the arterial wall. A new insight into the role of collagen accumulation in plaque development has been gained by understanding the role of extracellular matrix (ECM).[5] ECM composition and its metabolic behaviour are decisive factors in the evolution and complications of atherosclerosis. It is evident that the metabolic balance of ECM is regulated in large part by matrix metalloproteinases (MMPs).[5]

LOX-1, a lectin-like receptor for ox-LDL, is a major receptor responsible for binding, internalization, and degradation of ox-LDL in endothelial cells.[6] It has been demonstrated that insertion of LOX-1 plasmids in cardiac fibroblasts that are naturally low expressors of LOX-1 alters the biology of fibroblasts to pro-inflammatory phenotype.[7] Further, ox-LDL treatment enhances collagen formation by fibroblasts that can be blocked by anti-LOX-1 antibody. In cultured cardiac myocytes, LOX-1 activation has also been shown to upregulate the expression of pro-collagen I and collagen type I via redox-sensitive pathways.[8] A recent study shows that LOX-1 deletion alters signals of myocardial

† These authors contributed equally to this work.
* Corresponding author. Tel: +1 501 686 5046; fax: +1 501 686 6180.
E-mail address: mehtaJL@uams.edu

remodelling immediately after ischaemia.[9] These observations collectively suggest that LOX-1 may be an important player in the regulation of ECM.

There is growing evidence to support the contributory role of LOX-1 in atherogenesis.[6] Importantly, targeted deletion of LOX-1 reduces atherogenesis in the LDL receptor knockout (LDLR KO) mice fed high-cholesterol diet.[10] In order to gain further insight into the role of LOX-1 in ECM formation in atherogenesis, we studied the effect of LOX-1 deletion on ECM accumulation and MMPs expression in atherosclerotic aortas. We also examined the modulation of oxidative stress and pro-inflammatory signals as the mechanistic basis of ECM modulation.

2. Methods

2.1 Animal protocol

The generation of LOX-1 KO and LOX-1/LDLR double KO mice has been described recently.[10] In brief, C57BL/6 mice (also referred to as wild-type mice) and homozygous LDLR KO mice (on C57BL/6 background) were originally obtained from Jackson Laboratories. The homozygous LOX-1 KO and LOX-1/LDLR double KO mice were backcrossed eight times with C57BL/6 strain to replace the genetic background. C57BL/6 and homozygous LOX-1 KO, LDLR KO and LDLR/LOX-1 double KO (all on C57BL/6 background) mice were bred by brother–sister mating and housed in the breeding colony at University of Arkansas for Medical Sciences, Little Rock, AR, USA. All male animals were given a high-cholesterol diet (4% cholesterol/10% cocoa butter) for 18 weeks from the age of 6 weeks. This investigation conforms to the Guidelines for the Care and Use of Laboratory Animals published by the US National Institutes of Health. All experimental procedures were performed in accordance with protocols approved by the Institutional Animal Care and Usage Committee.

2.2 Quantitative analysis of collagen-positive area

Entire aortas from the aortic arch above the aortic valves to the iliac bifurcation were harvested and embedded in paraffin. Cross-sections (5 μm thick) were made at five pre-defined points (proximal ascending aorta, aortic arch, descending aorta, mid-thoracic aorta, and abdominal aorta above the renal arteries).[10] The sections were stained with Masson's trichrome and Picro-sirius red. The images were captured by digital imaging system and analysed with Image pro software (Media Cybernetics). The presence of area positive for collagen (blue) was recorded for each section, averaged for each mouse and expressed as ratio of entire vessel wall area. Data were obtained from five mice in each group.

2.3 Immunohistochemical staining

Sections (5 μm thick) of aortas made at five pre-defined points as described above were incubated with primary antibody to fibronectin, osteopontin, or nitrotyrosine (Santa Cruz, dilution 1:200) for 2 h at room temperature, rinsed with PBS, and incubated with corresponding biotinylated secondary antibody for 30 min. The slides were then incubated in avidin–biotin complex for 30 min followed by rinse with PBS, then incubated in diaminobenzidine, and finally washed in distilled water and counterstained with hematoxylin.

2.4 Protein preparation and analysis by western blot

Aortic specimens were derived from animals at 18 weeks of high-cholesterol diet. Aortic protein was extracted for expression analysis of pro-collagen I, osteopontin, fibronectin, MMP-2, MMP-9, NADPH oxidase $p22^{phox}$, NADPH oxidase $p47^{phox}$, NADPH oxidase $gp91^{phox}$, NADPH oxidase Nox-4, nitrotyrosine, Akt-1, phos-Akt-1 (Ser 473), phos-S1177 endothelial nitric oxide synthase (eNOS), haem-oxygenase-1 (HO-1), and β-actin using standard methodologies of western blot.[8] Band density relative to β-actin was analysed.

2.5 MMP-2 and MMP-9 activity assay

Activity of MMP-2 and MMP-9 in aortic tissues was determined by zymography.[8]

2.6 Statistical analysis

Data are presented as mean ± SE. All data were analysed by a two-way ANOVA with a Bonferroni *post hoc* test. Four-fold comparisons were performed and an adjusted value of $P < 0.05$ was considered to be significant. All calculations were performed with SPSS version 12.0.

3. Results

3.1 LOX-1 deletion reduces collagen deposition in the aortic wall

Collagen is an important component of atherosclerotic plaque, and its role as a component of ECM has been established.[5] We, therefore, determined accumulation of collagen by specific staining in multiple aortic sections from different animal groups. The results of Masson's trichrome and Picro-sirius red staining were similar. Representative examples of aortic sections are shown in *Figure 1A*, and the summary data from Masson's trichrome staining are shown in *Figure 2A*. There was extensive deposition of collagen in the aortas of LDLR KO mice, encompassing ~40% of the aortic cross-sectional area. In comparison to the LDLR KO mice, collagen deposition was much less in the aorta of double KO mice (~50% reduction vs. LDLR KO mice, $P < 0.01$). The wild-type control mice also showed some collagen-positive areas (~18% of cross-sectional area), perhaps a result of high-cholesterol diet feeding, and that there were much fewer collagen-positive areas in the LOX-1 KO mice.

In support of the collagen accumulation data, the LDLR KO mice showed a marked increase in pro-collagen I expression ($P < 0.01$ vs. wild-type mice). Deletion of LOX-1 in the LDLR KO mice reduced pro-collagen I expression ($P < 0.01$ vs. LDLR KO mice). Importantly, the pro-collagen I expression was lower in the LOX-1 KO mice when compared with that in the wild-type mice ($P < 0.01$, *Figure 2B*), indicating that LOX-1 deletion also reduces the basal expression of pro-collagen I.

3.2 LOX-1 deletion reduces expression of osteopontin and fibronectin in the aortic wall

Osteopontin has been shown to interact with fibronectin and to play an important role in ECM organization and stability.[11] Accordingly, we determined the expression of osteopontin and fibronectin in the aortic sections from different groups of mice. Representative examples (immunohistochemistry) are shown in *Figures 1B* and western analysis in *Figure 3*. The expression of osteopontin as well as fibronectin was increased in the LDLR KO mice ($P < 0.01$ vs. wild-type mice). In contrast, LDLR/LOX-1 double KO mice showed much less increase in the expression of osteopontin as well as fibronectin ($P < 0.01$ vs. LDLR KO mice).

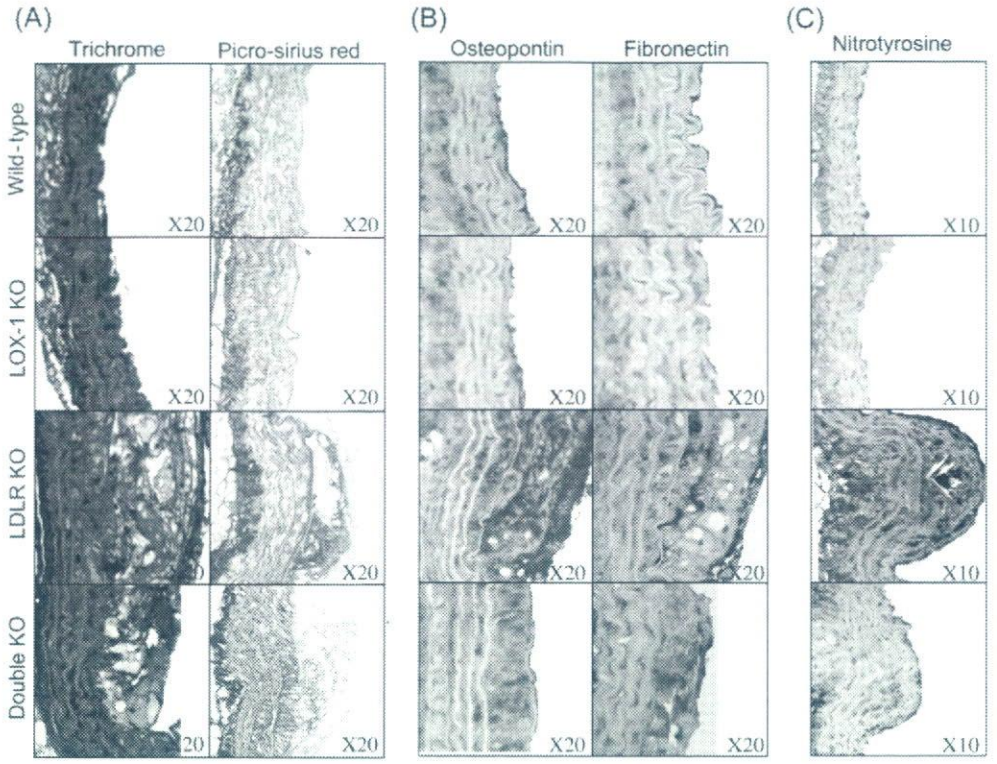

Figure 1 Representative examples of collagen accumulation (Picro-sirius and Masson's trichrome staining, *A*), osteopontin and fibronectin expression, *B*, and nitrotyrosine staining, *C*) in selected aortic sections.

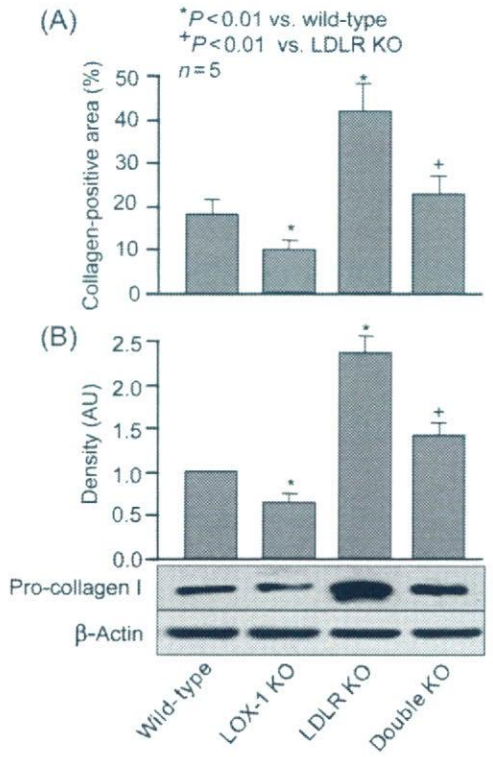

Figure 2 Quantitation of collagen accumulation (*A*) and expression of pro-collagen I by western blot analysis (*B*). KO, knockout.

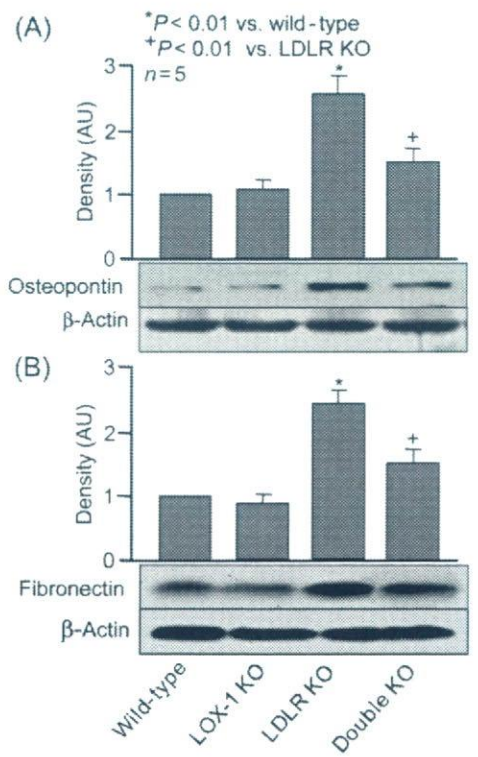

Figure 3 Representative examples and quantitation of expression of osteopontin (*A*) and fibronectin (*B*), determined by western blot analysis.

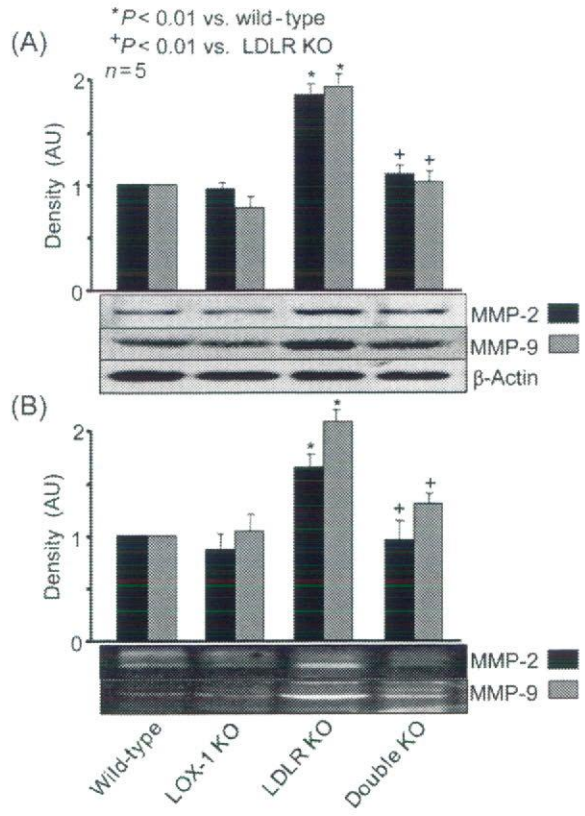

Figure 4 Representative examples and quantitation of expression of matrix metalloproteinases (MMPs), determined by western blot analysis (*A*) and of MMP activity, determined by zymography (*B*).

3.3 LOX-1 deletion reduces matrix metalloproteinases expression and activity in the aortic wall

Collagen accumulation in various tissues depends not only on its production, but also on its degradation by proteinases, such as MMPs.[12] Therefore, we determined the expression and activity of mouse-specific MMP-2 and MMP-9 (*Figure 4A* and *B*). The expression as well as activity of MMP-2 and MMP-9 was found to be increased ≈100% in LDLR KO ($P <$ 0.01 vs. wild-type mice). On the other hand, deletion of LOX-1 in the LDLR KO mice 'normalized' the expression and activity of MMPs ($P < 0.01$ vs. LDLR KO mice; $P > 0.05$ vs. wild-type mice).

3.4 LOX-1 deletion reduces redox-sensitive signalling associated with collagen accumulation

Atherosclerosis involves oxidative stress and inflammation.[13,14] In keeping with this concept, $p47^{phox}$, $p22^{phox}$, $gp91^{phox}$, and Nox-4 subunits of NADPH oxidase were markedly increased in the LDLR KO mice ($P < 0.01$ vs. wild-type mice) (*Figure 5A*). The upregulation of four subunits of NADPH oxidase was reduced by LOX-1 deletion in the LDLR KO mice. It is noteworthy that the expression of all four subunits of NADPH oxidase was lower in the LOX-1 KO mice ($P <$ 0.01 vs. wild-type mice), indicating that LOX-1 deletion reduces the basal expression of four subunits of NADPH oxidase. To confirm the increased production of reactive oxidative species (ROS) in aorta, we examined the presence of nitrotyrosine as an indirect marker of oxidative stress by immunohistochemistry (*Figure 1C*) and western blot analysis

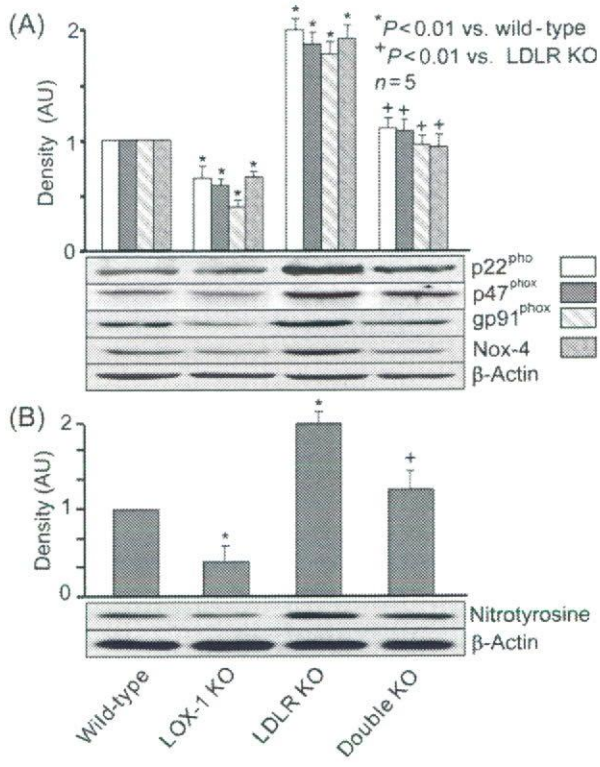

Figure 5 Representative examples and quantitation of the expression of NADPH oxidases ($p47^{phox}$, $p22^{phox}$, $gp91^{phox}$, and Nox-4 subunits) (*A*) and nitrotyrosine (*B*), determined by western blot analysis.

(*Figure 5B*). Expression of nitrotyrosine was higher in LDLR KO mice ($P < 0.01$ vs. the wild-type mice), and LOX-1 deletion limited this increase in nitrotyrosine expression.

Next, we studied the expression of Akt-1 protein and its phosphorylation in the aortic tissues. While Akt-1 protein expression was similar in all mice, Akt-1 phosphorylation was reduced by 50% in the LDLR KO mice ($P < 0.01$ vs. wild-type mice), and LOX-1 deletion in the wild-type and LDLR KO mice 'normalized' Akt-1 phosphorylation (*Figure 6A*).

Akt-1 activation regulates the activity of eNOS. We, therefore, examined phos-S1177 eNOS expression in the aortic tissues. As shown in *Figure 6B*, the expression of phos-S1177 eNOS was reduced by ~50% in the LDLR KO mice compared with the wild-type mice ($P < 0.01$), and LOX-1 deletion markedly increased eNOS phosphorylation in the LDLR mice ($P < 0.01$). It is of note that the basal level of eNOS activity was higher in the LOX-1 KO mice when compared with wild-type mice ($P < 0.01$).

We also examined the expression of HO-1, another vasodilator species that is relevant in atherogenesis.[15,16] As shown in *Figure 6C*, HO-1 expression was reduced in the aortas from LDLR KO mice (vs. wild-type mice). On the other hand, LOX-1 deletion enhanced HO-1 expression in LDLR KO mice. As with eNOS activity, basal levels of HO-1 were higher in the LOX-1 KO mice (vs. wild-type mice, $P < 0.01$).

4. Discussion

Atherosclerosis has been viewed as uncontrolled plaque growth eventually leading to total occlusion of the artery. New clinical findings suggest that acute coronary events are triggered by thrombosis associated with rupture of the

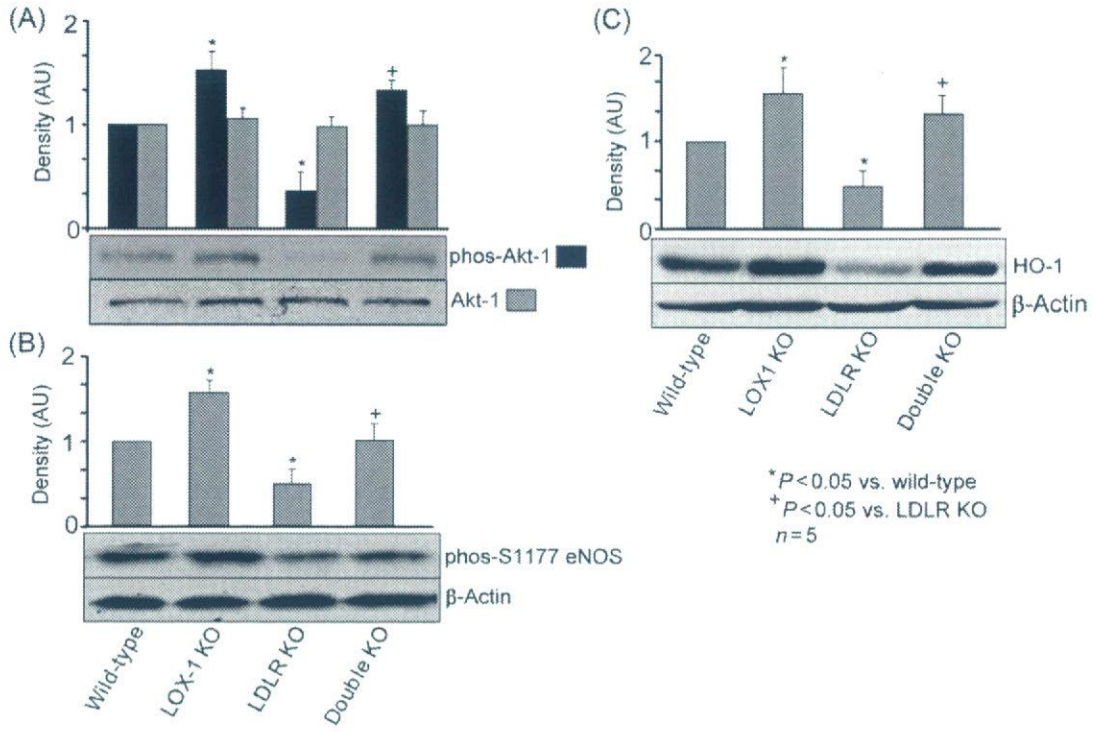

Figure 6 Representative examples and quantitation of the expression of Akt-1 (*A*), phos-S1177 eNOS (*B*), and HO-1 (*C*), determined by western blot analysis. eNOS, endothelial nitric oxide synthase; HO-1, haem-oxygenase-1; phos, phosphorylated.

atherosclerotic plaque.[17] Clinical data from analysis of human atherosclerotic regions by intravascular ultrasound histology and polarization-sensitive optical coherence tomography suggest that collagen deposition (fibrous tissue) is a significant component of the atherosclerotic region.[18,19] Detailed analysis of the atherosclerotic plaques in animal tissues also shows that collagen constitutes over 50% of the plaques.[20] It may be postulated that fibrous tissue provides an anchor for smooth muscle cells and monocytes/macrophages. In light of our previous *in vitro* studies[7] showing that collagen formation by fibroblasts treated with ox-LDL is an oxidant-response that can be blocked by LOX-1 abrogation, we embarked on this *in vivo* study to examine if LOX-1 deletion in the LDLR KO mice will attenuate collagen deposition. Indeed, our study shows that collagen deposition is markedly reduced in the LDLR KO mice with LOX-1 deletion. Further, this study revealed that the signals involved in collagen deposition in atherosclerotic tissues are similar to those seen in *in vitro* studies.

4.1 Collagen formation and deposition

While almost all cell types in atherosclerotic regions form collagen, fibroblasts are the primary source of collagen. Our previous studies showed that treatment of fibroblasts with ox-LDL enhances collagen formation, especially when LOX-1 is over-expressed in fibroblasts.[7] Treatment of fibroblasts with angiotensin II (Ang II), which is abundantly present in the atherosclerotic regions,[21] also stimulates fibroblast growth and collagen formation.[22] In addition to collagen formation, there is abundance of collagen degrading enzymes, the MMPs, in the atherosclerotic plaque.[5] Collagen degradation products and MMPs can also be identified in plasma and urine of patients with atherosclerosis.[23] However, these markers lack a specific 'tissue signature'.[20]

Simultaneous increase in MMPs and collagen expression in atherosclerotic tissues suggests that the two processes are inter-related and represent a cellular attempt to regulate the remodelling process. The expression of both MMPs and collagen may be a response to ROS release, a common accompaniment of atherogenesis.[13] We have earlier shown that atherosclerosis is associated with over-expression of LOX-1, a finding reproduced in the LDLR KO mice on high-fat diet.[10] It is of note that LOX-1 activation has been linked to ox-LDL, Ang II, and release of ROS.[6]

We showed that LOX-1 deletion reduced the extent of atherosclerosis in the LDLR KO mice,[10] and also attenuated the expression/activity of MMPs and pro-collagen I. Reduction in pro-collagen I may represent a decrease in oxidant stress in the LOX-1 KO mice. NADPH oxidase is the major source of ROS in the vascular tissues.[24] We measured the expression of NADPH oxidase and nitrotyrosine, and found that the expression of NADPH oxidase ($p22^{phox}$, $p47^{phox}$, $pg91^{phox}$, and Nox-4 subunits) and nitrotyrosine was increased dramatically in the LDLR KO mice. This increase in NADPH oxidase and nitrotyrosine (oxidant stress marker) was much less in mice with LOX-1 deletion.

We do not know the exact source of NADPH oxidase and ROS in the atherosclerotic arteries, but it could be fibroblasts, smooth muscle cells, endothelial cell, and/or inflammatory cells. All these cell types have been shown to generate ROS;[24] it also appeared to be confirmed by nitrotyrosine staining in our study (*Figure 1C*).

4.2 Osteopontin and fibronectin expression in atherosclerosis

We observed that the expression of osteopontin as well as fibronectin was increased in the aortas of LDLR KO mice compared with wild-type mice. Osteopontin has been

implicated in chemoattraction of monocytes and in cell-mediated immunity.[25] It is also important in smooth muscle cell migration.[26] Collins *et al.*[27] showed that osteopontin was formed in response to Ang II, and the osteopontin null mice had much less fibroblasts proliferation and much less ECM accumulation after 3 weeks of Ang II infusion. Interestingly, osteopontin null mice also had reduced atherosclerosis and MMPs activity.[28]

The signal for osteopontin expression seems to involve oxidant stress and related pathways. Xie *et al.*[29] showed that Ang II regulates osteopontin gene expression via ROS-sensitive signalling pathway. Lai *et al.*[30] demonstrated that osteopontin, via activation of NADPH oxidase-derived superoxide anion formation, promotes upregulation of MMP-9 in primary aortic myofibroblasts and smooth muscle cells under hyperglycaemic conditions *in vitro*. Gorin *et al.*[31] have similarly shown a relationship between NADPH oxidase activation and fibronectin generation in both *in vitro* and *in vivo* conditions. Our previous study[10] showed that p38MAPK activity is increased in the LDLR KO mice and much less so in the LDLR KO mice with LOX-1 deletion. The results of the present study coupled with previous work suggest a strong link between NADPH oxidase-induced oxidant stress, osteopontin/fibronectin expression, and MMPs expression. In keeping with these studies, it was not surprising that the expression of osteopontin, fibronectin, and MMPs was lower in the aortas of mice with LOX-1 abrogation that had low levels of NADPH oxidase ($p22^{phox}$, $p47^{phox}$, $gp91^{phox}$, and Nox-4 subunits).

4.3 Endothelial nitric oxide synthase and HO-1 in atherosclerosis and the effect of LOX-1 deletion

Atherosclerotic regions have reduced activity of eNOS.[32] This phenomenon was confirmed in the present study (*Figure 6*) as well as in our previous work.[10] Reduction of locally released NO may enhance oxidative stress and subsequently monocyte accumulation, collagen synthesis, and cell proliferation. Protein kinase B/Akt-1 is important in downstream targeting of extracellular PI-3 kinase signalling, and alterations in its activity may be important in the phosphorylation of NOS in response to oxidant stimuli.[33] In keeping with this concept, we observed a reduction in Akt-1 phophorylation and diminished expression of eNOS in the aortas of LDLR KO mice. Importantly, LOX-1 deletion enhanced Akt-1 phosphorylation to a level higher than that in the wild-type mice. Previous *in vivo* studies have also documented that LOX-1 is key to altered endothelium-dependent vasorelaxation in atherosclerosis.[10]

There is emerging evidence that HO-1 and its products function as adaptive molecules against oxidative insults.[15,16] HO-1 upregulation in turn reduces NADPH oxidase activity[34] and NF-κB phosphorylation.[35] The signalling of HO-1 in atherogenesis is not clear, but it appears that persistent oxidant stress may reduce the expression of HO-1.[36] There is also evidence that Akt-1 activation upregulates HO-1.[37] The absence of HO-1 exacerbates atherosclerotic lesion formation,[38] suggesting a potential tissue protective role for HO-1 in atherogenesis. In keeping with these observations, we found that atherosclerotic aortas from LDLR KO mice had reduced expression of HO-1. With LOX-1 deletion, there was a marked increase in HO-1 expression. Whether the two events are related or not is not clear, but our observations strongly suggest that oxidant stress and HO-1 are intertwined, and Akt-1/ NF-κB phosphorylation may relate to these alterations.

4.4 Collagen deposition in atherosclerosis and its relevance to LOX-1 deletion

Enhanced expression of collagen appears to be an inherent part of the atherosclerotic process. A host of mediators of oxidative stress, including ox-LDL and Ang II, are present in the atherosclerotic regions and activate NADPH oxidase system. The intense oxidant stress in the atherosclerotic regions stimulates MAPKs and the redox-sensitive transcription factors, such as NF-κB[10] followed by upregulation of genes, such as fibronectin, osteopontin, collagen, and MMPs, which result in the formation of collagen. Interestingly, excessive collagen deposition is associated with enhanced release of MMPs. While ox-LDL and Ang II-stimulated LOX-1 activation enhances oxidative stress and inflammation,[6] and oxidative stress *per se* upregulates LOX-1 expression.[6] This process may self-amplify leading to intense collagen deposition in atherosclerotic regions over time. These events are summarized in *Figure 7*.

Attenuation of the expression of the redox-sensitive signals and collagen formation with LOX-1 deletion suggests that LOX-1 could be a relevant therapeutic target in the management of atherosclerosis and vascular remodelling process.

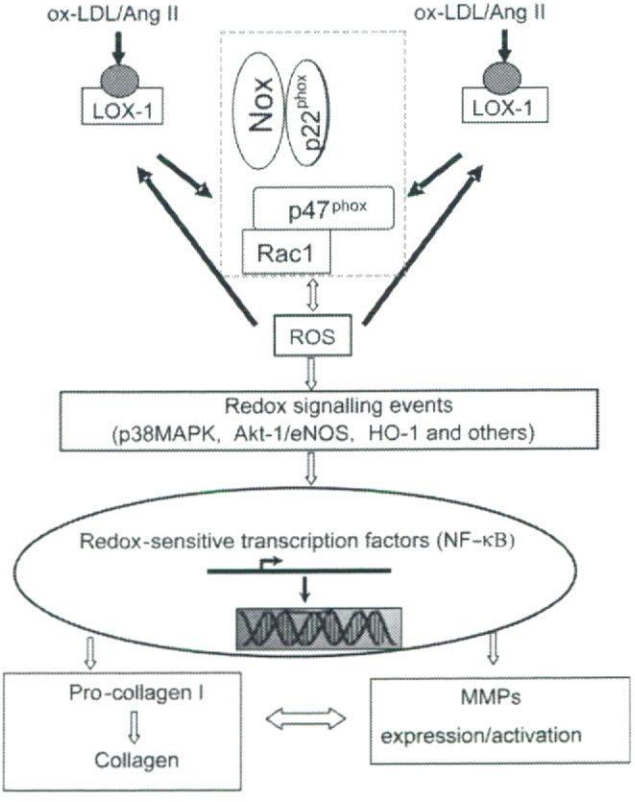

Figure 7 Hypothesized pathways of LOX-1-mediated collagen and MMPs. Mediators of oxidative stress, including oxidized LDL (ox-LDL) and angiotensin II (Ang II), induce LOX-1 expression and resultant activation of NADPH oxidase and reactive oxygen species (ROS) generation. ROS in turn upregulates LOX-1 expression. ROS causes activation of MAPKs followed by transcription of redox-sensitive transcription factor/s which induce the gene for collagen. MMPs are activated as auto-regulatory response to collagen synthesis.

Conflict of interest: none declared.

Funding

This study was supported in part by funds from the Department of Veterans Affairs (J.L.M.), and the Ministry of Education, Culture, Sports, Science and Technology of Japan; the Ministry of Health, Labour and Welfare of Japan; and the National Institute of Biomedical Innovation, Japan (T.S.).

References

1. Steinberg D. Lipoproteins and the pathogenesis of atherosclerosis. *Circulation* 1987;**76**:508-514.
2. Ross R, Glomset JA. Atherosclerosis and the arterial smooth muscle cell. Proliferation of smooth muscle is a key event in the genesis of the lesions of atherosclerosis. *Science* 1973;**180**:1332-1339.
3. Libby P. Inflammatory and immunomechanism in atherogenesis. *Atheroscler Rev* 1990;**21**:79-89.
4. Schulze PC, Lee RT. Oxidative stress and atherosclerosis. *Curr Atheroscler Rep* 2005;**7**:242-248.
5. Kunz J. Matrix metalloproteinases and atherogenesis in dependence of age. *Gerontology* 2007;**53**:63-73.
6. Mehta JL, Chen J, Hermonat PL, Romeo F, Novelli G. Lectin-like oxidized-low density lipoprotein receptor-1 (LOX-1): a critical player in the development of atherosclerosis and related disorders. *Cardiovasc Res* 2006;**69**:36-45.
7. Chen K, Chen J, Liu Y, Xie J, Li D, Sawamura T *et al.* Adhesion molecule expression in fibroblasts: alteration in fibroblast biology after transfection with LOX-1 plasmids. *Hypertension* 2005;**46**:622-627.
8. Hu CP, Dandapat A, Liu Y, Hermonat PL, Mehta JL. Blockade of hypoxia-reoxygenation-mediated collagen type I expression and MMP activity by over-expression of TGFβ1 in mouse cardiomyocytes. *Am J Physiol Heart Circ Physiol* 2007;**293**:H1833-H1838.
9. Hu CP, Dandapat A, Chen J, Fujita Y, Inoue N, Kawase Y *et al.* LOX-1 deletion alters signals of myocardial remodeling immediately after ischemia-reperfusion. *Cardiovasc Res* 2007;**76**:292-302.
10. Mehta JL, Sanada N, Hu CP, Chen J, Dandapat A, Sugawara F *et al.* Deletion of LOX-1 reduces atherogenesis in LDLR knockout mice fed high cholesterol diet. *Circ Res* 2007;**100**:1634-1642.
11. Kossmehl P, Schonberger J, Shakibaei M, Faramarzi S, Kurth E, Habighorst B *et al.* Increase of fibronectin and osteopontin in porcine hearts following ischemia and reperfusion. *J Mol Med* 2005;**83**:626-637.
12. Heeneman S, Cleutjens JP, Faber BC, Creemers EE, van Suylen R-J, Lutgens E *et al.* The dynamic extracellular matrix: intervention strategies during heart failure and atherosclerosis. *J Pathol* 2003;**200**: 516-525.
13. Schulze PC, Lee RT. Oxidative stress and atherosclerosis. *Curr Atheroscler Rep* 2005;**7**:242-248.
14. Reiss AB, Glass AD. Atherosclerosis: immune and inflammatory aspects. *J Investig Med* 2006;**54**:123-131.
15. Morita T. Heme-oxygenase and atherosclerosis. *Arterioscler Thromb Vasc Biol* 2005;**25**:1786-1795.
16. Wu BJ, Kathir K, Witting PK, Beck K, Choy K, Li C *et al.* Antioxidants protect from atherosclerosis by a heme oxygenase-1 pathway that is independent of free radical scavenging. *J Exp Med* 2006;**203**:1117-1127.
17. Shin J, Edelberg JE, Hong MK. Vulnerable atherosclerotic plaque: clinical implications. *Curr Vasc Pharmacol* 2003;**1**:183-204.
18. Herbert CS, Chandler AB, Dinsmore RE, Fuster V, Glagov S, Insull W *et al.* A definition of advanced types of atherosclerotic lesions and a histological classification of atherosclerosis. *Circulation* 1995;**92**:1355-1374.
19. Nadkarni SK, Pierce MC, Park BH, de Boer JF, Whittaker P, Bouma BE *et al.* Measurement of collagen and smooth muscle cell content in atherosclerotic plaques using polarization-sensitive optical coherence tomography. *J Am Coll Cardiol* 2007;**49**:1474-1481.
20. Rekhter M. Vulnerable atherosclerotic plaque: emerging challenge for animal models. *Curr Opin Cardiol* 2002;**17**:626-632.
21. Chen J, Li D, Schaefer R, Mehta JL. Cross-talk between dyslipidemia and renin-angiotensin system and the role of LOX-1 and MAPK in atherogenesis studies with the combined use of rosuvastatin and candesartan. *Atherosclerosis* 2006;**184**:295-301.
22. Chen K, Chen J, Li D, Zhang X, Mehta JL. Angiotensin II regulation of collagen type I expression in cardiac fibroblasts: modulation by PPAR-gamma ligand pioglitazone. *Hypertension* 2004;**44**:655-661.
23. Risteli J, Risteli L. Analysing connective tissue metabolites in human serum. Biochemical, physiological and methodological aspects. *J Hepatol* 1995;**22**:77-81.
24. Becker LB. New concepts in reactive oxygen species and cardiovascular reperfusion physiology. *Cardiovasc Res* 2004;**61**:461-470.
25. Ogawa D, Stone JF, Takata Y, Blaschke F, Chu VH, Towler DA *et al.* Liver x receptor agonists inhibit cytokine-induced osteopontin expression in macrophages through interference with activator protein-1 signaling pathways. *Circ Res* 2005;**96**:e59-e67.
26. Renault MA, Jalvy S, Belloc I, Pasquet S, Sena S, Olive M *et al.* AP-1 is involved in UTP-induced osteopontin expression in arterial smooth muscle cells. *Circ Res* 2003;**93**:674-681.
27. Collins AR, Schnee J, Wang W, Kim S, Fishbein MC, Bruemmer D *et al.* Osteopontin modulates angiotensin II-induced fibrosis in the intact murine heart. *J Am Coll Cardiol* 2004;**43**:1698-1705.
28. Bruemmer D, Collins AR, Noh G, Wang W, Territo M, Arias-Magallona S *et al.* Angiotensin II-accelerated atherosclerosis and aneurysm formation is attenuated in osteopontin-deficient mice. *J Clin Invest* 2003;**112**: 1318-1331.
29. Xie Z, Singh M, Singh K. ERK1/2 and JNKs, but not p38 kinase, are involved in reactive oxygen species-mediated induction of osteopontin gene expression by angiotensin II and interleukin-1beta in adult rat cardiac fibroblasts. *J Cell Physiol* 2004;**198**:399-407.
30. Lai C-F, Seshadri V, Huang K, Shao J-S, Cai J, Vattikuti R *et al.* An osteopontin-NADPH oxidase signaling cascade promotes pro-matrix metalloproteinase 9 activation in aortic mesenchymal cells. *Circ Res* 2006;**98**:1479-1489.
31. Gorin Y, Block K, Hernandez J, Bhandari B, Wagner B, Barnes JL *et al.* Nox4 NAD(P)H oxidase mediates hypertrophy and fibronectin expression in the diabetic kidney. *J Biol Chem* 2005;**280**:39616-39626.
32. Kawashima S, Yokoyama M. Dysfunction of endothelial nitric oxide synthase and atherosclerosis. *Arterioscler Thromb Vasc Biol* 2004;**24**: 998-1005.
33. Michell BJ, Griffiths JE, Mitchelhill KI, Rodriguez-Crespo I, Tiganis T, Bozinovski S *et al.* The Akt kinase signals directly to endothelial nitric oxide synthase. *Curr Biol* 1999;**9**:845-848.
34. Colombrita C, Lombardo G, Scapagnini G, Abraham NG. Heme oxygenase-1 expression levels are cell cycle dependent. *Biochem Biophys Res Commun* 2003;**308**:1001-1008.
35. Seldon MP, Silva G, Pejanovic N, Larsen R, Gregoire IP, Filipe J *et al.* Heme oxygenase-1 inhibits the expression of adhesion molecules associated with endothelial cell activation via inhibition of NF-kappaB RelA phosphorylation at serine 276. *J Immunol* 2007;**179**:7840-7851.
36. Hoekstra KA, Godin DV, Kurtu J, Cheng KM. Effects of oxidant-induced injury on heme oxygenase and glutathione in cultured aortic endothelial cells from atherosclerosis-susceptible and -resistant Japanese quail. *Mol Cell Biochem* 2003;**254**:61-71.
37. Hsu JT, Kan WH, Hsieh CH, Choudhry MA, Schwacha MG, Bland KI *et al.* Mechanism of estrogen-mediated attenuation of hepatic injury following trauma-hemorrhage: Akt-dependent HO-1 up-regulation. *J Leukoc Biol* 2007;**82**:1019-1026.
38. Yet SF, Layne MD, Liu X, Chen YH, Ith B, Sibinga NE *et al.* Absence of heme oxygenase-1 exacerbates atherosclerotic lesion formation and vascular remodeling. *FASEB J* 2003;**17**:1759-1761.

Modulation of Angiotensin II–Mediated Hypertension and Cardiac Remodeling by Lectin-Like Oxidized Low-Density Lipoprotein Receptor-1 Deletion

Changping Hu, Abhijit Dandapat, Liuqin Sun, Muhammad R. Marwali, Nobutaka Inoue, Fumiaki Sugawara, Kazuhiko Inoue, Yosuke Kawase, Kou-ichi Jishage, Hiroshi Suzuki, Paul L. Hermonat, Tatsuya Sawamura, Jawahar L. Mehta

Abstract—Angiotensin II via type 1 receptor activation upregulates the expression of lectin-like oxidized low-density lipoprotein receptor-1 (LOX-1), and LOX-1 activation, in turn, upregulates angiotensin II type 1 receptor expression. We postulated that interruption of this positive feedback loop might attenuate the genesis of angiotensin II–induced hypertension and subsequent cardiac remodeling. To examine this postulate, LOX-1 knockout and wild-type mice were infused with angiotensin II or norepinephrine (control for angiotensin II) for 4 weeks. Angiotensin II–, but not norepinephrine-, induced hypertension was attenuated in LOX-1 knockout mice. Angiotensin II–induced cardiac remodeling was also attenuated in LOX-1 knockout mice. Importantly, angiotensin II type 1 receptor expression was reduced, and the expression and activity of endothelial NO synthase were preserved in the tissues of LOX-1 knockout mice given angiotensin II. Reactive oxygen species generation, nicotinamide-adenine dinucleotide phosphate oxidase expression, and phosphorylation of p38 and p44/42 mitogen-activated protein kinases were also much less pronounced in the LOX-1 knockout mice given angiotensin II. These alterations in biochemical and structural abnormalities were associated with preservation of cardiac hemodynamics in the LOX-1 knockout mice. To confirm that fibroblast function is modulated in the absence of LOX-1, cardiac fibroblasts from wild-type and LOX-1 knockout mice were treated with angiotensin II. Indeed, LOX-1 knockout mice cardiac fibroblasts revealed an attenuated profibrotic response on treatment with angiotensin II. These observations provide strong evidence that LOX-1 is a key modulator of the development of angiotensin II–induced hypertension and subsequent cardiac remodeling. (***Hypertension*. 2008;52:556-562.)**

Key Words: angiotensin ■ hypertension ■ cardiac remodeling ■ LOX-1 ■ oxidative stress

Cardiac remodeling is initially an adaptive response to several forms of cardiac stress states, such as hypertension. Sustained remodeling results in heart failure and is a powerful independent risk factor for cardiac morbidity and mortality.[1] Therefore, identification of the molecular mechanisms involved in cardiac remodeling is an important challenge for the cardiovascular biologists.

The renin-angiotensin system and its effector hormone, angiotensin II (Ang II), have well-known endocrine properties that contribute to cardiac remodeling and heart failure. Previous studies have shown that Ang II via type 1 receptor (AT1R) activation stimulates the expression of lectin-like oxidized low-density lipoprotein receptor-1 (LOX-1).[2] In turn, activation of LOX-1 upregulates AT1R expression.[3] Activation of both AT1R and LOX-1 induces a state of oxidative stress.[4] In addition, activation of both AT1R and LOX-1 enhances the growth of cardiac fibroblasts and promotes collagen synthesis.[5,6]

Although LOX-1 mRNA expression is minimal in normal arterial tissues, it is markedly upregulated in vascular tissues of spontaneously hypertensive animals, suggesting a correlation between LOX-1 and hypertension.[7] This concept is supported by in vitro observations that Ang II upregulates LOX-1 expression,[2] and angiotensin-converting enzyme inhibitors and AT1R blockers decrease LOX-1 expression.[8] These findings suggest that LOX-1 overexpression may contribute to the pathological states induced by Ang II. We postulated that interruption of the positive feedback loop between Ang II and LOX-1 might reduce the genesis of Ang II–induced hypertension and subsequent cardiac remodeling.

Received April 22, 2008; first decision May 12, 2008; revision accepted June 26, 2008.

From the Department of Medicine and Physiology and Biophysics (C.H., A.D., L.S., M.R.M., P.L.H., T.S., J.L.M.), University of Arkansas for Medical Sciences and Central Arkansas Veterans Healthcare System, Little Rock; Department of Pharmacology (C.H.), School of Pharmaceutical Sciences, Central South University, Changsha, China; Department of Ophthalmology (L.S.), Heping Hospital, Changzhi Medical College, Changzhi, China; Department of Vascular Physiology (N.I., F.S., K.I., T.S.), National Cardiovascular Center Research Institute, Osaka, Japan; Chugai Research Institute for Medical Science (Y.K., K-i.J.), Shizuoka, Japan; and Obihiro University of Agriculture and Veterinary Medicine (H.S.), Hokkaido, Japan.

The first 2 authors contributed equally to this work.

Correspondence to Jawahar L. Mehta, Cardiovascular Medicine, University of Arkansas for Medical Sciences, 4301 W Markham St, Slot 532, Little Rock, AR 72205-7199. E-mail MehtaJL@uams.edu

***Hypertension* is available at http://hyper.ahajournals.org** **DOI: 10.1161/HYPERTENSIONAHA.108.115287**

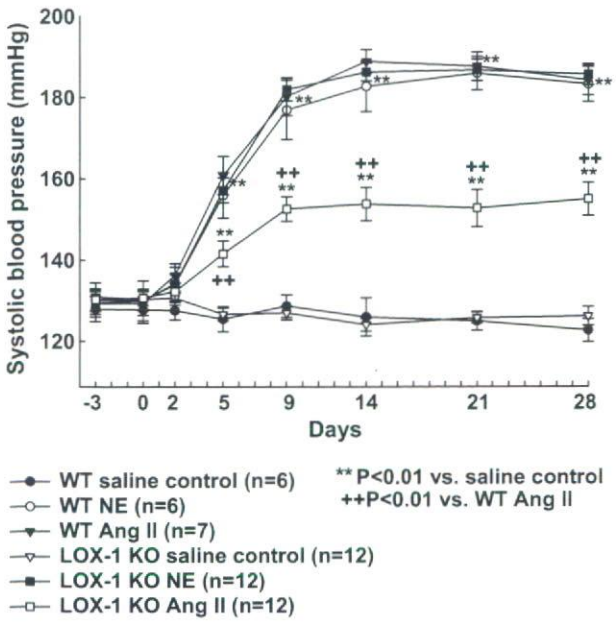

Figure 1. Systolic blood pressure rise in response to Ang II and norepinephrine (NE) infusion in wild-type (WT) and LOX-1 KO mice. LOX-1 deletion selectively attenuated blood pressure response to Ang II, but not NE, infusion.

To address this issue, we used a mouse model of LOX-1 deficiency (hereafter called LOX-1 knockout or KO mice).

Our specific aims were to examine the following hypotheses: (1) LOX-1 blockade (use of LOX-1 KO mice) will attenuate Ang II–induced hypertension; (2) cardiac remodeling after Ang II infusion will be less in the LOX-1 KO mice; and (3) fibroblasts from LOX-1 KO mice will generate less collagen (versus wild-type mice) when exposed to Ang II.

Materials and Methods

LOX-1 KO and wild-type mice were infused with Ang II (50 ng/min) or norepinephrine (100 ng/min) for 4 weeks. Blood pressure, cardiac remodeling, and oxidative stress sensitive signaling were determined. For details, please refer to the online data supplement (http://hyper.ahajournals.org). Data are expressed as means±SEs. All of the data were analyzed by a 2-way ANOVA with a Bonferroni posthoc test. A $P<0.05$ was considered significant.

Results

Blood Pressure and Cardiac Hemodynamics in Response to Ang II or Norepinephrine

Basal systolic blood pressure was similar in the wild-type and LOX-1 KO mice and remained unchanged in all of the saline-treated mice for the duration of the study. On the other hand, systolic blood pressure exhibited a progressive increase during the infusion (with Ang II or norepinephrine) period, reaching a peak value on day 14 and remaining at plateau through day 28 in the wild-type mice (Figure 1). The rise in blood pressure was much less in the LOX-1 KO mice compared with that in wild-type mice ($P<0.01$), despite infusion with the same dose of Ang II. In contrast to the effect of Ang II, norepinephrine infusion caused a similar rise in blood pressure in wild-type and LOX-1 KO mice for the duration of the study. Thus, LOX-1 deletion resulted in a selective attenuation of blood pressure in response to Ang II.

At the end of Ang II or norepinephrine infusion, we measured left ventricular hemodynamics. As shown in Figure S1, heart rate, left ventricular systolic pressure, left ventricular end-diastolic pressure, and the first derivatives of the pressure over time were similar in all of the mice, indicating that the basal hemodynamics were comparable in wild-type and LOX-1 KO mice. Ang II or norepinephrine infusion had no significant effect on heart rate in wild-type and LOX-1 KO mice but induced a marked increase in left ventricular systolic pressure, left ventricular end-diastolic pressure, and first derivatives of the pressure over time compared with corresponding saline-treated control mice ($P<0.01$). It is of note that the increase in left ventricular systolic pressure, left ventricular end-diastolic pressure, and first derivatives of the pressure over time was much less in LOX-1 KO mice compared with that in the wild-type mice despite infusion of a similar dose of Ang II ($P<0.05$). Norepinephrine-induced hemodynamic changes remained similar in wild-type and LOX-1 KO mice.

Cardiac Remodeling After Sustained Hypertension and Effect of LOX-1 Deletion

Hearts from wild-type and LOX-1 KO mice were assessed with regard to their susceptibility to hypertrophic response to sustained hypertension. Chronic Ang II, as well as norepinephrine infusion, induced significant cardiac hypertrophy (expressed as a ratio of heart weight to body weight or to tibia length) in wild-type and LOX-1 KO mice (Figure 2A through 2C; $P<0.01$ versus corresponding saline-treated mice). The cardiomyocyte cross-sectional area also increased in response to sustained hypertension (Figure 2D and 2E). Ang II–induced cardiac hypertrophy was much less in the LOX-1 KO mice compared with that in wild-type mice ($P<0.01$), as evidenced from a smaller increase in the heart weight and cross-sectional area of cardiomyocytes.

On the other hand, there was no significant difference in cardiac hypertrophy in response to norepinephrine infusion between wild-type and LOX-1 KO mice. This is in keeping with a similar degree of hypertensive response to norepinephrine in both groups of animals.

Because the increase in cardiac mass and cardiomyocyte size is accompanied by induction of specific genes, atrial natriuretic peptide (ANP) and α-tubulin,[9,10] we sought to measure their expression. As shown in Figure 3A and Figure S2, the expression of ANP and α-tubulin was increased in wild-type mice given Ang II or norepinephrine compared with saline-infused wild-type mice ($P<0.01$). Importantly, the LOX-1 KO mice demonstrated much less induction of ANP and α-tubulin despite Ang II infusion ($P<0.01$ versus Ang II–infused wild-type mice). This phenomenon was confirmed by immunohistochemical staining for α-tubulin (Figure 3B). Again, norepinephrine-induced induction of ANP and α-tubulin remained similar in wild-type and LOX-1 KO mice.

Sustained hypertension and resultant cardiac remodeling are characterized by abundant accumulation of matrix proteins in the extracellular space.[11] We, therefore, determined the accumulation of collagen in multiple sections of hearts from different animal groups. Results of Masson trichrome

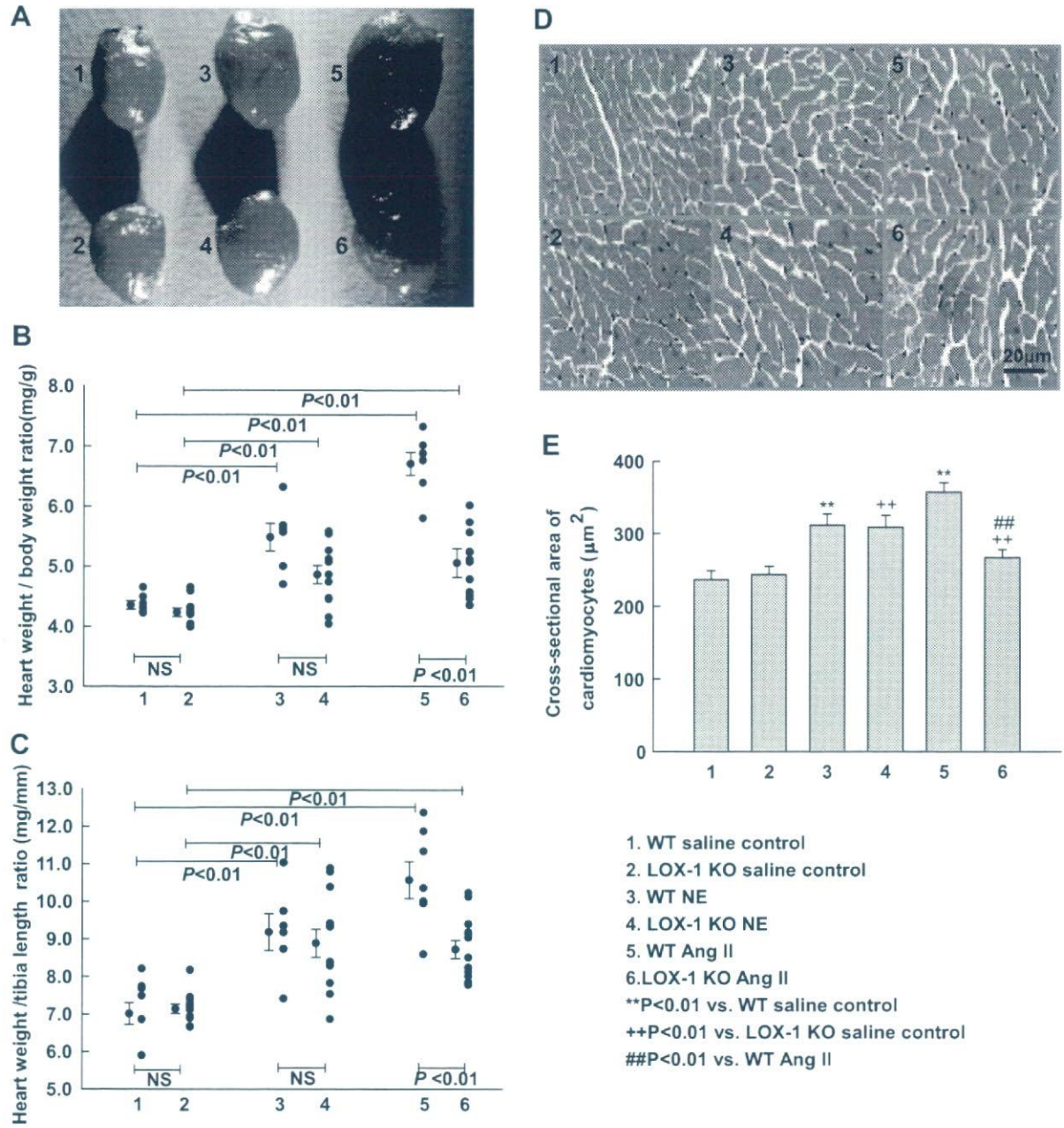

Figure 2. Cardiac hypertrophy in mice given Ang II and NE. A, Representative images of cardiac hypertrophy (bar=1 mm). B, Heart weight:body weight ratio (n=6 to 12). C, Heart weight:tibia length ratio (n=6 to 12). D, Representative images of hematoxylin-eosin micrographs of cardiomyocyte cross-sections (magnification, ×200). E, Summarized data on cardiomyocyte size (n=6). LOX-1 deletion reduced cardiac hypertrophy selectively in response to Ang II infusion.

and Picrosirius red staining were similar. Representative examples are shown in Figure 3B, and the summary data from trichrome staining are shown in Figure 3C. In the wild-type mice, sustained hypertension after Ang II or norepinephrine infusion resulted in a significant increase in collagen accumulation ($P<0.01$ versus saline-infused wild-type mice). In contrast, the LOX-1 KO mice exhibited much less increase in collagen accumulation despite Ang II infusion ($P<0.01$ versus Ang II–infused wild-type mice). Norepinephrine-induced collagen accumulation remained similar in wild-type and LOX-1 KO mice (Figure 3B and 3C).

Collagen type I, derived from its precursor procollagen I, is considered a major determinant of myocardial stiffness.[11] Osteopontin has been shown to interact with fibronectin and plays an important role in left ventricular remodeling.[12] Therefore, we determined the expression of procollagen I, osteopontin, and fibronectin in mice hearts. As shown in Figure 3A, the expression of procollagen I, osteopontin, and fibronectin increased significantly after infusion of Ang II or norepinephrine in the wild-type mice ($P<0.01$ versus saline-infused wild-type mice). However, LOX-1 KO mice given Ang II infusion exhibited much less increase in the expression of procollagen I, osteopontin, and fibronectin in the LOX-1 KO mice ($P<0.01$ versus wild-type mice). The expression of procollagen I, osteopontin, and fibronectin induced by norepinephrine infusion was similar in wild-type

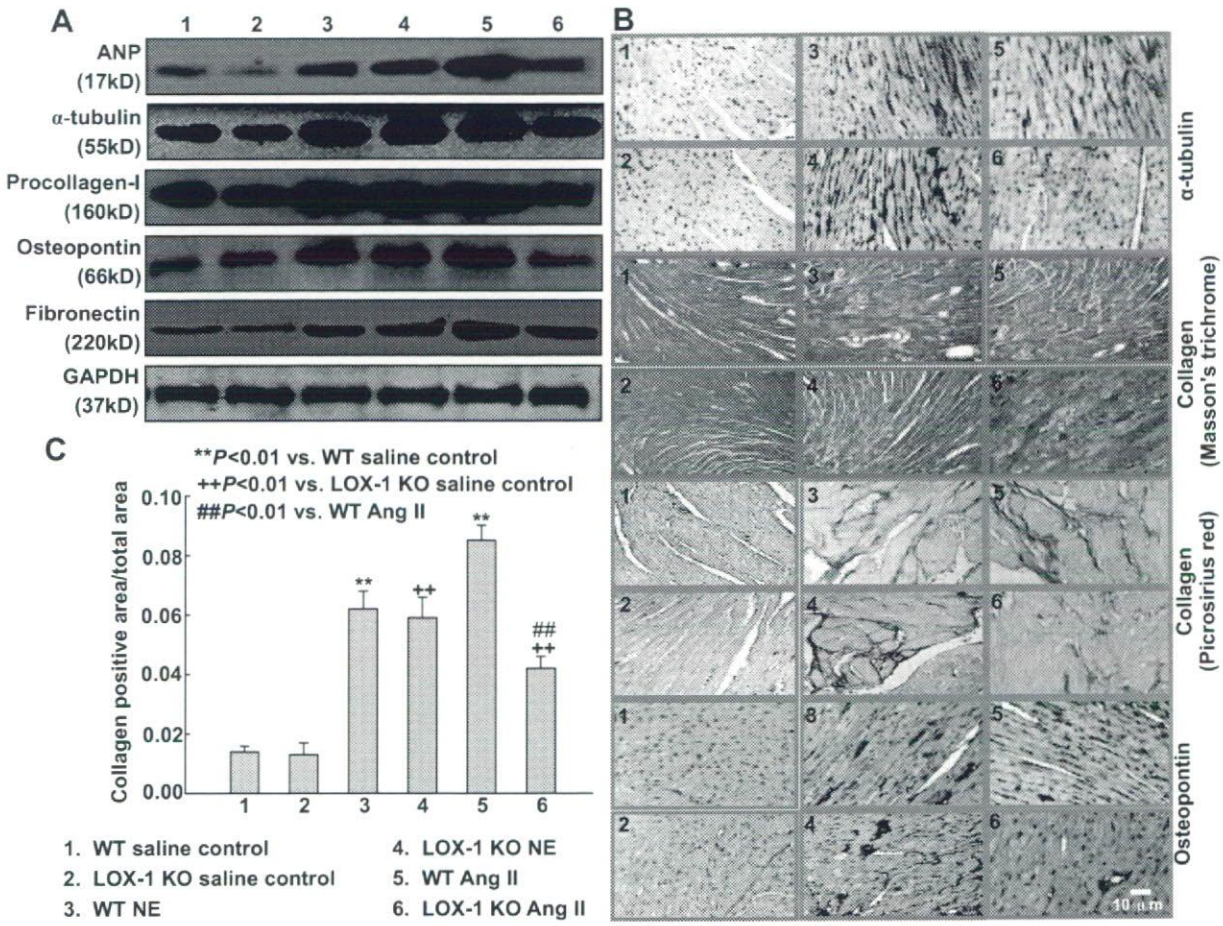

Figure 3. Markers of cardiac hypertrophy (ANP and α-tubulin) and fibrosis (collagen, procollagen-I, osteopontin, and fibronectin) in mice given Ang II and NE. A, Representative Western blot. B, Immunostaining of α-tubulin, collagen, and osteopontin. C, Summary of data on trichrome staining. These markers of cardiac remodeling were less pronounced in LOX-1 KO mice given Ang II. Data are representative of 4 experiments.

and LOX-1 KO mice. We also performed immunohistochemical staining for osteopontin in heart sections, and the data were consistent with the results by Western analysis (Figure 3B).

Expression of AT1R and Endothelial NO Synthase Induced by Ang II Infusion and the Effect of LOX-1 Deletion

Most of the cardiovascular actions of Ang II have been attributed to AT1R activation, whereas the hypertensive response to norepinephrine is related to α_1-adrenoceptor activation.[13,14] We, therefore, determined the expression of AT1R and α_1-adrenoceptors. As shown in Figure 4A and Figure S3, AT1R expression increased in the aortic and cardiac tissues after infusion of Ang II in the wild-type mice ($P<0.01$ versus saline-infused wild-type mice). However, Ang II-infused LOX-1 KO mice exhibited much less increase in AT1R expression ($P<0.01$ versus wild-type mice). Interestingly, the expression of α_1-adrenceptors induced by norepinephrine infusion remained similar in aortic and cardiac tissues from wild-type and LOX-1 KO mice (Figure 4B).

Our recent study has shown that endothelium-dependent relaxation of aorta, as well as endothelial NO synthase (eNOS) expression, is preserved in the LOX-1 KO mice fed a high-cholesterol diet.[15] In the present study, we measured the expression of eNOS and phosphorylated S1177-eNOS in the aorta and found that wild-type mice given Ang II had low levels of eNOS and phosphorylated S1177-eNOS ($P<0.01$ versus control mice). Importantly, LOX-1 deletion preserved the expression of eNOS and phosphorylated S1177-eNOS despite Ang II infusion ($P<0.01$; Figure 4C). It is of note that the downregulation of eNOS and phosphorylated eNOS expression induced by norepinephrine infusion remained similar in aortas from wild-type and LOX-1 KO mice (Figure 4C).

Oxidative Stress Induced by Ang II and Norepinephrine and the Effect of LOX-1 Deletion

Oxidative stress and resultant release of reactive oxygen species (ROS) have been linked to the development of cardiac remodeling and progression to heart failure.[16] Ang II also upregulates LOX-1 expression.[2] Therefore, we determined nicotinamide-adenine dinucleotide phosphate (NADPH) oxidase ($p47^{phox}$ and $p22^{phox}$ subunits) expression, ROS production, phosphorylation of oxidative stress–sensitive mitogen-activated protein kinases (MAPKs; p38 and p44/42 MAPK isoforms), and LOX-1 expression. In keeping with previous in vitro studies,[17] Ang II infusion induced oxidative stress (dichlorofluorescein fluorescence, 8-isoprostane in hearts, serum malondialdehyde, and $p47^{phox}$

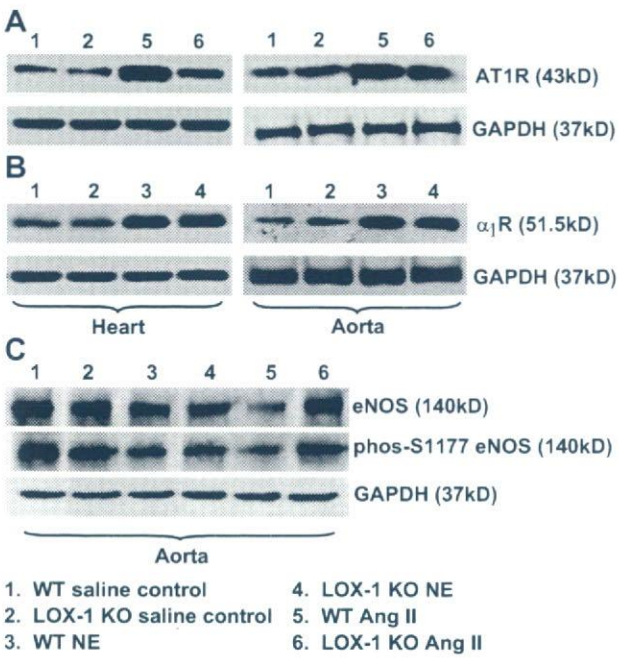

Figure 4. Expression of AT1R, α_1-adrenoceptor (α1R), and eNOS in mice given Ang II and norepinephrine (NE). LOX-1 deletion caused attenuation of AT1R expression and enhancement of eNOS expression/activity in response to Ang II. The expression of α1R and eNOS in response to NE was not affected by LOX-1 deletion.

and $p22^{phox}$ subunits, Figure 5A through 5D) in the wild-type mice, but much less so in the LOX-1 KO mice. Norepinephrine infusion also increased oxidative stress in the wild-type mice, but it was not affected by LOX-1 deletion.

As shown in Figure 5D and Figure S4, protein levels of p38 and p44/42 MAPKs were unchanged in response to Ang II and norepinephrine infusion, but their phosphorylation increased significantly during Ang II infusion ($P<0.01$ versus saline-infused wild-type mice). Importantly, Ang II-infused LOX-1 KO mice exhibited much less phosphorylation of MAPKs ($P<0.01$ versus Ang II–infused wild-type mice). However, the increased phosphorylation of MAPKs during norepinephrine infusion was not affected by LOX-1 deletion.

In keeping with previous in vitro studies,[2] Ang II infusion enhanced LOX-1 expression in the wild-type mice (Figure 5D). As expected, LOX-1 was not detectable in LOX-1 KO mice hearts. Importantly, LOX-1 expression was only minimally upregulated by norepinephrine infusion.

Studies in Cultured Cardiac Fibroblasts

Fibroblasts form a significant component of cardiac mass, and their growth and activity (collagen formation) contribute to cardiac remodeling.[5,6,11] To mimic the in vivo state, we treated mouse cardiac fibroblasts with Ang II (1 μmol/L) for 24 hours. Prolonged exposure of cardiac fibroblasts from wild-type mice to Ang II induced dichlorofluorescein fluorescence and NADPH oxidase ($p47^{phox}$ and $p22^{phox}$ subunits) expression, but these changes were much less pronounced in fibroblasts from LOX-1 KO mice despite their treatment with Ang II ($P<0.01$). In addition, phosphorylation of p38 and p44/42 MAPK, which was quite marked in the fibroblasts from wild-type mice, was less in fibroblasts from LOX-1 KO mice despite their exposure to Ang II (Figure S5).

Treatment with Ang II for 24 hours also increased procollagen I expression in cardiac fibroblasts from wild-type mice, but to a much smaller extent in fibroblasts from LOX-1 KO mice (Figure S6). These data are consistent with the data on collagen staining in the hearts from wild-type and LOX-1 KO mice. LOX-1 expression was also quite marked in cardiac fibroblasts isolated from wild-type mice. As expected, fibroblasts isolated from LOX-1 KO mice showed the absence of LOX-1 (Figure S6).

Discussion

We show that LOX-1 deletion attenuated Ang II–induced hypertension and cardiac remodeling. Most importantly, our in vitro studies confirmed that fibroblasts from LOX-1 KO mice generated much less collagen (versus wild-type mice) when exposed to Ang II.

Ang II via AT1R activation upregulates LOX-1 through redox-sensitive pathways,[18] and activation of LOX-1 upregulates AT1R expression.[3] We, accordingly, postulated that Ang II and LOX-1 operate in a positive feedback fashion with the common theme being generation of ROS and activation of MAPKs. To examine the relevance of this postulate in the in vivo state, we measured blood pressure response to Ang II in wild-type mice and studied the role of LOX-1 abrogation by using the LOX-1 KO mice. In these LOX-1 KO mice, endothelium-dependent relaxation, as well as eNOS generation, is preserved when the animals are fed a high-cholesterol diet.[15] In the present study, we observed that, whereas the resting blood pressure was similar in the LOX-1 KO and wild-type mice, blood pressure rise in response to Ang II was markedly attenuated in the LOX-1 KO mice. Interestingly, AT1R expression increased in the wild-type mice given Ang II infusion, as observed by others as well.[19] The expression and activity of eNOS both decreased in the wild-type mice given Ang II. Importantly, the LOX-1 KO mice given Ang II infusion exhibited a much smaller increase in the expression of AT1R and a marked upregulation of eNOS expression/activity compared with the wild-type mice. These findings confirm that the Ang II-AT1R-LOX-1 loop is an important regulator of blood pressure.

The blood pressure increase in response to norepinephrine was not affected by LOX-1 abrogation. It is of note that norepinephrine infusion caused only a minimal change in LOX-1 expression (versus a large increase in Ang II–infused mice). Norepinephrine infusion, as expected, increased α_1-adrenoceptor expression, and LOX-1 deletion did not affect α_1-adrenoceptor upregulation. LOX-1 deletion also had no effect on the downregulation of eNOS expression/activity induced by norepinephrine infusion. As such, it is not surprising that the norepinephrine-α_1-adrenoceptor-hypertension pathway was not affected by LOX-1 deletion. Many studies have shown that Ang II causes ROS generation by activating NADPH oxidases,[16,17] which, in turn, activate p38 and/or p44/42 MAPKs and redox-sensitive transcription factors.[17] This process influences downstream signals, resulting in cardiomyocyte hypertrophy and procollagen synthesis.[11,16,17] Activation of this cascade has been thought to lead

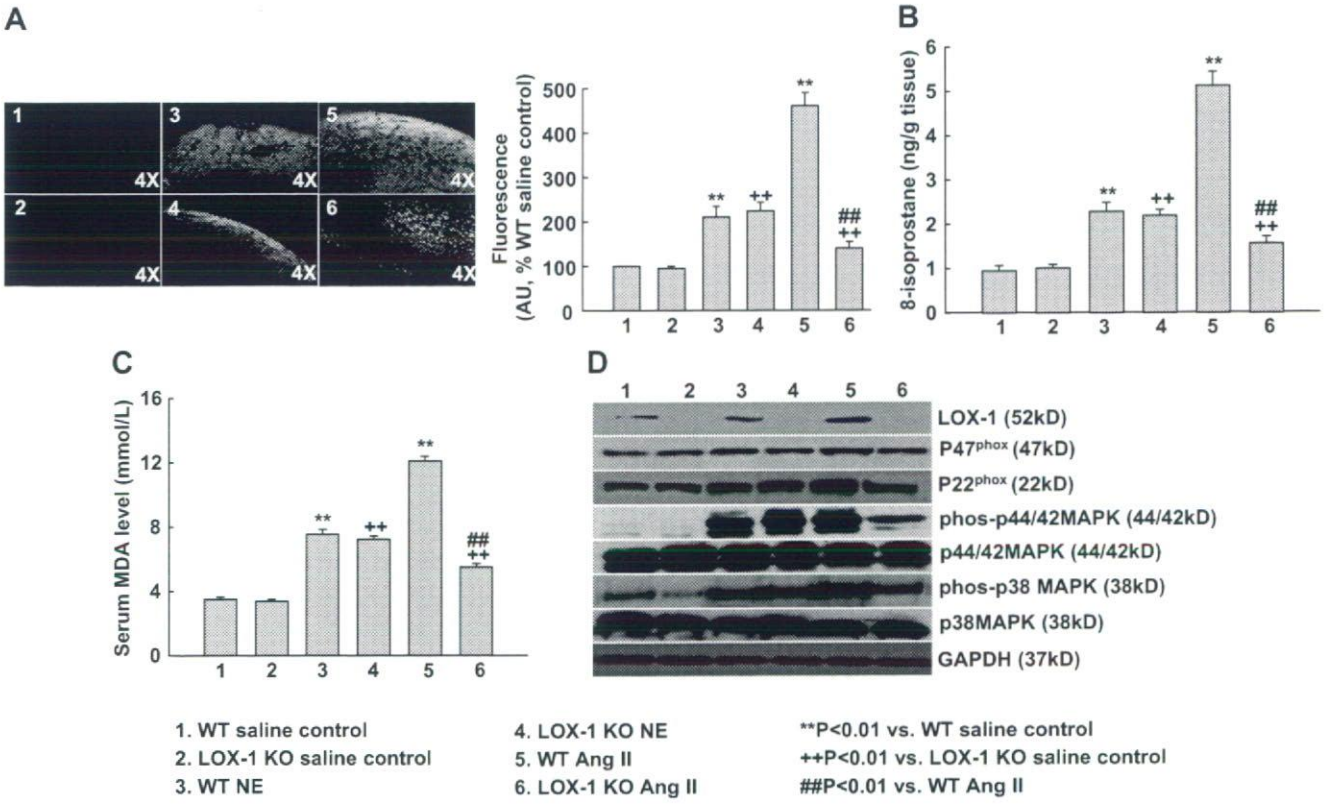

Figure 5. Oxidative stress and LOX-1 expression in mice given Ang II or NE. A, Representative dichlorofluorescein fluorescence images indicating reactive oxygen species release in heart and the summary of fluorescence data (n=5). B, Cardiac 8-iosprostane level (n=5). C, Serum malondialdehyde (MDA) levels (n=5). Note the marked dichlorofluorescein fluorescence in Ang II–infused wild-type (WT) mice heart; the fluorescence was attenuated in LOX-1 KO mice hearts. Norepinephrine (NE) infusion caused much less fluorescence (vs Ang II infusion), and LOX-1 deletion had no effect. D, Representative Western blots. Ang II, but not NE, infusion increased LOX-1 expression in WT mice. Both NE and Ang II enhanced phosphorylation of p38 and p44/42 MAPKs in WT mice. LOX-1 deletion reduced phosphorylation of MAPKs selectively in response to Ang II but not NE. This Western blot is representative of 4 separate experiments.

to the development of cardiac remodeling in sustained hypertension.[16] This concept is supported by the observations that the NADPH oxidase inhibitor apocynin reduces blood pressure elevation and prevents vascular remodeling in Ang II–infused mice. Furthermore, hydralazine, which decreases blood pressure but does not affect ROS and related pathways, has no effects on vascular remodeling induced by Ang II.[20]

We observed that prolonged infusion of Ang II, as well as norepinephrine, increased heart weight in the wild-type mice. The increase in heart weight was a manifestation of cardiomyocyte hypertrophy, because cardiomyocyte cross-sectional area and α-tubulin and ANP expression in the heart were enhanced. In addition, there was clear evidence of fibroblast proliferation and collagen accumulation. It is worth noting that the cardiomyocyte hypertrophy and fibrosis were greater in Ang II–infused mice as compared with norepinephrine-infused mice, perhaps an indication of greater ROS generation in response to Ang II despite a similar degree of blood pressure elevation (Figure 1). Ang II–infused LOX-1 KO mice exhibited a very low level of ROS generation and downstream signal activation. It was, therefore, not surprising that LOX-1 KO mice had much less cardiomyocyte hypertrophy and collagen deposition (versus the wild-type mice) despite infusion of same doses of Ang II. The LOX-1 KO mice given norepinephrine infusion did not exhibit any significant changes in ROS generation and downstream signaling, and, hence, showed no change in cardiomyocyte hypertrophy and fibrosis. Previous studies have demonstrated that LOX-1 is a key modulator of cardiac remodeling, which starts immediately after a brief period of ischemia reperfusion via ROS-dependent pathways, and that the signals of cardiac remodeling are attenuated in the LOX-1 KO mice.[21]

We also found that the expression of osteopontin, as well as fibronectin, increased in the wild-type mice given Ang II and norepinephrine. Osteopontin has been shown to interact with fibronectin and plays an important role in matrix organization and stability.[12] Previous studies also showed that Ang II increases osteopontin expression, and the osteopontin null mice given Ang II infusion have much less cardiac fibrosis and hypertrophy.[22,23] Xie et al[24] showed that the signals for Ang II–induced osteopontin expression also involve oxidative stress and resultant p42/44 MAPK activation. Gorin et al[25] have similarly shown a relationship between NADPH oxidase activation and fibronectin generation both in vitro and in vivo. In keeping with these studies, we found that the expression of procollagen I, as well as osteopontin and fibronectin, was lower in the hearts of Ang II–treated LOX-1 KO mice that had low levels of oxidant stress and activation of MAPKs.

The data on cultured cardiac fibroblasts exposed to Ang II in vitro support the in vivo observations in mice given Ang II

infusion. The fibroblasts from LOX-1 KO mice revealed much less oxidative stress and activation of MAPKs compared with fibroblasts from wild-type mice after exposure to Ang II. In keeping with previous studies in rodent cardiac fibroblasts,[5,17] Ang II exposure induced procollagen I expression, but the procollagen I expression was decreased by LOX deletion. Chen et al[6] showed that the overexpression of LOX-1 in rat cardiac fibroblasts enhances the expression of collagen I and the phosphorylation of p38 MAPK. These observations further suggest that the Ang II (AT1R)-ROS-LOX-1 loop might directly regulate the development of cardiac remodeling in mice with an Ang II–induced increase in blood pressure.

Perspectives

This study provides exciting in vivo evidence of a positive feedback loop between Ang II-ROS-LOX-1, which results in the syndrome of chronic sustained hypertension, and cardiac remodeling. The in vitro component using cardiac fibroblasts from LOX-1 KO and wild-type mice lends support to this concept. Our study does not allow us to dissociate the direct effect of LOX-1 deletion on cardiac hypertrophy from its blood pressure–attenuating effects. Therefore, the role of LOX-1 in the regulation of cardiac remodeling needs to be further investigated in other models of pressure or volume overload or in primary cultured cardiomyocytes.

Sources of Funding

This study was supported by funds from the Department of Veterans Affairs (J.L.M.) and a grant from the American Heart Association (P.L.H.); the Ministry of Education, Culture, Sports, Science, and Technology of Japan (T.S.); the Ministry of Health, Labor, and Welfare of Japan (T.S.); and the National Institute of Biomedical Innovation, Japan (T.S.).

Disclosures

None.

References

1. Hilfiker-Kleiner D, Landmesser U, Drexler H. Molecular mechanisms in heart failure. Focus on cardiac hypertrophy, inflammation, angiogenesis, and apoptosis. *J Am Coll Cardiol*. 2006;48:A56–A66.
2. Chen J, Liu Y, Liu H, Hermonat PL, Mehta JL. Molecular dissection of angiotensin II-activated human LOX-1 promoter. *Arterioscler Thromb Vasc Biol*. 2006;26:1163–1168.
3. Li D, Saldeen T, Romeo F, Mehta JL. Oxidized LDL upregulates angiotensin II type 1 receptor expression in cultured human coronary artery endothelial cells: the potential role of transcription factor NF-kappaB. *Circulation*. 2000;102:1970–1976.
4. Mehta JL, Chen J, Hermonat PL, Romeo F, Novelli G. Lectin-like, oxidized low-density lipoprotein receptor-1 (LOX-1): a critical player in the development of atherosclerosis and related disorders. *Cardiovasc Res*. 2006;69:36–45.
5. Chen K, Mehta JL, Li D, Joseph L, Joseph J. Transforming growth factor beta receptor endoglin is expressed in cardiac fibroblasts and modulates profibrogenic actions of angiotensin II. *Circ Res*. 2004;95:1167–1173.
6. Chen K, Chen J, Liu Y, Xie J, Li D, Sawamura T, Hermonat PL, Mehta JL. Adhesion molecule expression in fibroblasts: alteration in fibroblast biology after transfection with LOX-1 plasmids. *Hypertension*. 2005;46:622–627.
7. Nagase M, Hirose S, Sawamura T, Masaki T, Fujita T. Enhanced expression of endothelial oxidized low-density lipoprotein receptor (LOX-1) in hypertensive rats. *Biochem Biophys Res Commun*. 1997;237:496–498.
8. Morawietz H, Rueckschloss U, Niemann B, Duerrschmidt N, Galle J, Hakim K, Zerkowski HR, Sawamura T, Holtz J. Angiotensin II induces LOX-1, the human endothelial receptor for oxidized low-density lipoprotein. *Circulation*. 1999;100:899–902.
9. Arimoto T, Takeishi Y, Takahashi H, Shishido T, Niizeki T, Koyama Y, Shiga R, Nozaki N, Nakajima O, Nishimaru K, Abe J, Endoh M, Walsh RA, Goto K, Kubota I. Cardiac-specific overexpression of diacylglycerol kinase zeta prevents Gq protein-coupled receptor agonist-induced cardiac hypertrophy in transgenic mice. *Circulation*. 2006;113:60–66.
10. Kee HJ, Sohn IS, Nam KI, Park JE, Qian YR, Yin Z, Ahn Y, Jeong MH, Bang YJ, Kim N, Kim JK, Kim KK, Epstein JA, Kook H. Inhibition of histone deacetylation blocks cardiac hypertrophy induced by angiotensin II infusion and aortic banding. *Circulation*. 2006;113:51–59.
11. Weber KT. Fibrosis, a common pathway to organ failure: angiotensin II and tissue repair. *Semin Nephrol*. 1997;17:467–491.
12. Kossmehl P, Schonberger J, Shakibaei M, Faramarzi S, Kurth E, Habighorst B, von Bauer R, Wehland M, Kreutz R, Infanger M, Schulze-Tanzil G, Paul M, Grimm D. Increase of fibronectin and osteopontin in porcine hearts following ischemia and reperfusion. *J Mol Med*. 2005;83:626–637.
13. Weiss D, Kools JJ, Taylor WR. Angiotensin II-induced hypertension accelerates the development of atherosclerosis in apoE-deficient mice. *Circulation*. 2001;103:448–454.
14. Cervenka L, Maly J, Karasova L, Simova M, Vitko S, Hellerova S, Heller J, El-Dahr SS. Angiotensin II-induced hypertension in bradykinin B2 receptor knockout mice. *Hypertension*. 2001;37:967–973.
15. Mehta JL, Sanada N, Hu CP, Chen J, Dandapat A, Sugawara F, Takeya M, Inoue K, Kawase Y, Jishage KI, Suzuki H, Satoh H, Schnackenberg L, Beger R, Hermonat PL, Thomas M, Sawamura T. Deletion of LOX-1 reduces atherogenesis in LDLR knockout mice fed high cholesterol diet. *Circ Res*. 2007;100:1634–1642.
16. Sorescu D, Griendling KK. Reactive oxygen species, mitochondria, and NAD(P)H oxidases in the development and progression of heart failure. *Congest Heart Fail*. 2002;8:132–140.
17. Chen J, Mehta JL. Angiotensin II-mediated oxidative stress and procollagen-1 expression in cardiac fibroblasts: blockade by pravastatin and pioglitazone. *Am J Physiol Heart Circ Physiol*. 2006;291:H1738–H1745.
18. Li D, Zhang YC, Philips MI, Sawamura T, Mehta JL. Upregulation of endothelial receptor for oxidized low-density lipoprotein (LOX-1) in cultured human coronary artery endothelial cells by angiotensin II type 1 receptor activation. *Circ Res*. 1999;84:1043–1049.
19. Harrison-Bernard LM, El-Dahr SS, O'Leary DF, Navar LG. Regulation of angiotensin II type 1 receptor mRNA and protein in angiotensin II-induced hypertension. *Hypertension*. 1999;33:340–346.
20. Virdis A, Neves MF, Amiri F, Touyz RM, Schiffrin EL. Role of NAD(P)H oxidase on vascular alterations in angiotensin II-infused mice. *J Hypertens*. 2004;22:535–542.
21. Hu CP, Dandapat A, Chen J, Fujita Y, Inoue N, Kawase Y, Jishage K, Suzuki H, Sawamura T, Mehta JL. LOX-1 deletion alters signals of myocardial remodeling immediately after ischemia-reperfusion. *Cardiovascular Res*. 2007;76:292–302.
22. Matsui Y, Jia N, Okamoto H, Kon S, Onozuka H, Akino M, Liu L, Morimoto J, Rittling SR, Denhardt D, Kitabatake A, Uede T. Role of osteopontin in cardiac fibrosis and remodeling in angiotensin II-induced cardiac hypertrophy. *Hypertension*. 2004;43:1195–1201.
23. Collins AR, Schnee J, Wang W, Kim S, Fishbein MC, Bruemmer D, Law RE, Nicholas S, Ross RS, Hsueh WA. Osteopontin modulates angiotensin II-induced fibrosis in the intact murine heart. *J Am Coll Cardiol*. 2004;43:1698–1705.
24. Xie Z, Singh M, Singh K. ERK1/2 and JNKs, but not p38 kinase, are involved in reactive oxygen species-mediated induction of osteopontin gene expression by angiotensin II and interleukin-1beta in adult rat cardiac fibroblasts. *J Cell Physiol*. 2004;198:399–407.
25. Gorin Y, Block K, Hernandez J, Bhandari B, Wagner B, Barnes JL, Abboud HE. Nox4 NAD(P)H oxidase mediates hypertrophy and fibronectin expression in the diabetic kidney. *J Biol Chem*. 2005;280:39616–39626.

Importance of Forkhead Transcription Factor Fkhl18 for Development of Testicular Vasculature

YUKO SATO,[1] TAKASHI BABA,[1] MOHAMAD ZUBAIR,[1] KANAKO MIYABAYASHI,[1] YOSHIRO TOYAMA,[2] MAMIKO MAEKAWA,[2] AKIKO OWAKI,[1] HIROFUMI MIZUSAKI,[1] TATSUYA SAWAMURA,[3] KIYOTAKA TOSHIMORI,[2] KEN-ICHIROU MOROHASHI,[1]* AND YUKO KATOH-FUKUI[1]

[1]*Division of Sex Differentiation, National Institute for Basic Biology, National Institutes of Natural Sciences, Okazaki, Japan*
[2]*Department of Anatomy, Graduate School of Medicine, Chiba University, Chiba, Japan*
[3]*Department of Vascular Physiology, National Cardiovascular Center Research Institute, Suita, Osaka, Japan*

ABSTRACT Forkhead transcription factors are characterized by a winged helix DNA binding domain, and the members of this family are classified into 20 subclasses by phylogenetic analyses. *Fkhl18* is structurally unique, and is classified into FoxS subfamily. We found *Fkhl18* expression in periendothelial cells of the developing mouse fetal testis. In an attempt to clarify its function, we generated mice with *Fkhl18* gene disruption. Although KO mice developed normally and were fertile in both sexes, we frequently noticed unusual blood accumulation in the fetal testis. Electron microscopic analysis demonstrated frequent gaps, measuring 100–400 nm, in endothelial cells of blood vessels. These gaps probably represented ectopic apoptosis of testicular periendothelial cells, identified by caspase-3 expression, in KO fetuses. No apoptosis of endothelial cells was noted. Fkhl18 suppressed the transcriptional activity of FoxO3a and FoxO4. Considering that *Fas ligand* gene expression is activated by Foxs, the elevated activity of Foxs in the absence of *Fkhl18* probably explains the marked apoptosis of periendothelial cells in *Fkhl18* KO mice. *Mol. Reprod. Dev.*

Key Words: forkhead; *Fkhl18*; gonad; periendothelial cells; endothelial cells; angiogenesis; vasculogenesis; fetal development

INTRODUCTION

There is a general agreement that gonad sex determination in mammals is a process initiated by *Sry* gene (sex-determining region of the Y chromosome; Koopman et al., 1990; Sinclair et al., 1990; Brennan and Capel, 2004). Downstream of *Sry*, *Sox9* (Sry-related HMG-box gene 9) specifies Sertoli cell lineages, organization of the testicular cord, and production of male hormones. In addition, the vasculature system develops differentially between the testis and ovary. Before the actions of *Sry* are evoked at around embryonic day 11.0 (E11.0), the structure of the primitive vasculature in the genital ridge is similar irrespective of sex. However, during the early phase of gonad sex differentiation, the mesonephric cells migrate vigorously into the developing testis to form a vasculature structure characteristic for the testis (Buehr et al., 1993; Martineau et al., 1997; Capel et al., 1999; Brennan et al., 2002, 2003). In contrast, no such active cell migration is observed in the developing fetal ovary. This difference gives rise to sexually dimorphic vascular patterns of the gonads. Particularly, in the testis, a large artery is formed at the coelomic surface at around E12.5. This male-specific vascular system that develops during fetal life is thought to be required for export of testosterone from the testis to the rest of the fetus to ensure masculinization (Renfree et al., 1995).

Vasculogenesis starts during fetal development. Precursor cells for blood vessel endothelia, which share origin with hematopoietic progenitors, assemble into a primitive vascular network of small capillaries. Subsequently, the vascular plexus progressively expands by sprouting and matures into stable blood vessels. During this phase of angiogenesis and arteriogenesis, nascent endothelial cells become covered by periendothelial cells

Grant sponsor: Ministry of Education, Culture, Sports Science, and Technology of Japan; Grant sponsor: Japan Science and Technology Corporation.

Yuko Sato's present address is Department of Vascular Physiology, National Cardiovascular Center Research Institute, Suita, Osaka 565-8565, Japan.

Mohamad Zubair's present address is Departments of Internal Medicine and Pharmacology, UT Southwestern Medical Center, Dallas, Texas 75390.

Hirofumi Mizusaki's present address is Department of Biochemistry, Nagasaki University School of Medicine, Nagasaki 852-8523, Japan.
Ken-Ichirou Morohashi's present address is Department of Molecular Biology, Graduate School of Medical Sciences, Kyushu University, Maidashi3-1-1, Higashi-Ku, Fukuoka 812-8582, Japan.

Yuko Katoh-Fukui's present address is Department of Aging Intervention, National Institute for Longevity Science, National Center for Geriatrics and Gerontology, Obu 474-8511, Japan.

*Correspondence to: Ken-Ichirou Morohashi, PhD, Division of Sex Differentiation, National Institute for Basic Biology, National Institutes of Natural Sciences, 5-1 Higashiyama, Myodaiji, Okazaki 444-8787, Japan. E-mail: moro@nibb.ac.jp

Received 2 December 2007; Accepted 18 December 2007
Published online in Wiley InterScience (www.interscience.wiley.com).
DOI 10.1002/mrd.20888

(pericytes and smooth muscle cells) and association with these cells is required to regulate proliferation, survival, migration, differentiation, vascular branching, blood flow, and vascular permeability (Carmeliet, 2003, 2005).

Forkhead (Fox) transcription factors carry a winged helix DNA-binding domain that share homology with their founding member forkhead protein in *Drosophila*. Phylogenic analysis of the forkhead domain consisting of highly conserved 100 amino acids led to placement of the family members into 20 subclasses, *FoxA* to *FoxS*. Foxs bind to consensus sequences, RYMAAYA (R = A or G; Y = C or T; M = A or C), as a monomer. Regions other than the conserved domain vary in terms of sequence and function. Some members act as transcriptional activators while others as repressors. Probably as transcriptional regulators, *Fox* genes are thought to play a variety of roles in fetal and adult tissues. In fact, gene knockout studies demonstrated that *Foxa2* is required for node and notochord formation, gastrulation, neural tube patterning, and gut morphogenesis (Ang and Rossant, 1994), *Foxi1/Fkh10* for inner ear development (Hulander et al., 1998, 2003), *Foxb1/Mf3* for the development of the diencephalon and midbrain, postnatal growth, and the milk-ejection reflex (Labosky et al., 1997), and *Foxc2/MFH1* for proliferation and patterning of paraxial mesoderm (Winnier et al., 1997).

Mutations in *FOX* genes have been linked to human diseases. Mutation of *FOXC1*, *FOXC2*, *FOXE1*, *FOXE3*, *FOXL2*, *FOXN1*, *FOXP2*, and *FOXP3* genes have been detected in various human congenital disorders (Mears et al., 1998; Frank et al., 1999; Chatila et al., 2000; Crisponi et al., 2001; Erickson et al., 2001; Lai et al., 2001; Semina et al., 2001; Brice et al., 2002; Castanet et al., 2002; Harris et al., 2002). Moreover, disordered expressions and functions of *FOX* genes were reported to correlate with carcinogenesis. For example, *FOXA1* gene is amplified and overexpressed in not all but certain esophageal and lung cancers (Lin et al., 2002). Likewise, in pancreatic cancer and basal cell carcinoma, *FOXM1* gene is upregulated due to transcriptional regulation by the Sonic Hedgehog (SHH) pathway (Teh et al., 2002). *FOXO1* gene is fused to *PAX3* or *PAX7* gene in rhabdomyosarcoma (Galili et al., 1993; Sorensen et al., 2002), while *FOXO3* and *FOXO4* genes are fused to myeloid/lymphoid or mixed-lineage leukemia (*MLL*) gene in hematological malignancies (Parry et al., 1994; Hillion et al., 1997). Several other studies demonstrated that these proteins are components of different signal transduction pathways, including those downstream of insulin, activin, and other transforming growth factor β-related ligands (Chen et al., 1996, 1997; Ogg et al., 1997; Nakae et al., 2002; Accili and Arden, 2004).

Fkhl18, a member of the *Fox* family, was originally identified by low-stringency screening of mouse (Kaestner et al., 1993) and human (Pierrou et al., 1994) genomic libraries. *Fkhl18* has low homology to other members of the Fox family, and is categorized under the *FoxS* subclass. However, its expression and function remain to be examined. In the present study, we demonstrated that *Fkhl18* is expressed in periendothelial cells and Sertoli cells of the developing fetal testis. We then generated the *Fkhl18*-deficient mouse to examine the physiological function of the gene product. Interestingly, the KO fetuses displayed affected testicular vasculature, suggesting that *Fkhl18* is involved in development of the fetal testis vasculature system.

MATERIALS AND METHODS

Reverse Transcription-Polymerase Chain Reaction (RT-PCR)

Total RNAs prepared from E16.5 fetal gonads were reverse-transcribed with Superscript II RNase H$^-$ Reverse Transcriptase (Invitrogen, San Diego, CA). PCR (94°C for 15 sec, 65°C for 30 sec, 68°C for 1 min, 30 cycles) was performed using the following primers for *Fkhl18* (NM_010226), Fkhl18-P1 (5′-CCC ACC AAG CCC CCT TAC AGC-3′) and Fkhl18-P2 (5′-GTC TGC GGC GAC GGA GAA AGC-3′), and for β-actin, β-actin-5′ (5′-ATG GAT GAC GAT ATC GCT-3′) and β-actin-3′ (5′-ATG GGT AGT CTG TCA GGT-3′).

In Situ Hybridization and Immunohistochemistry

E14.5 fetuses were fixed with 4% paraformaldehyde (PFA) at 4°C overnight and immersed in 30% sucrose. The fetuses were embedded in OCT compound and cryosectioned at 10 μm. The sections were treated with 1 mg/ml proteinase K (Merck, Tokyo, Japan) for 10 min at room temperature, acetylated and hybridized with 50 ng/ml riboprobe in 50% formamide, 5× SSC, 5 mM ethylenediaminetetraacetic acid (EDTA), 0.1% 3-[(3-cholamidopropyl) dimethylammonio]-1-propane sulfonate (CHAPS), 0.1% Tween-20, 0.2 mg/ml yeast tRNA, 0.1 mg/ml heparin sodium, and 1× Denhardt's solution, at 65°C. Thereafter, the sections were washed with 1× SSC containing 50% formaldehyde 30 min at 65°C. Digoxigenin (DIG)-labeled riboprobe (Roche Diagnostics, Mannheim, Germany) for full-length cDNA of *Fkhl18* was used. The DIG probes were visualized by alkaline phosphatase-conjugated anti-DIG antibody and NBT/BCIP reaction (Roche). Subsequently, some of the above sections were further subjected to immunohistochemistry using anti-*Ad4BP/SF-1* as described previously (Morohashi et al., 1994).

For immunohistochemistry, frozen sections were prepared from PFA-fixed E14.5 fetuses. The sections were dried and washed in phosphate buffered saline (PBS). After blocking with 2% skim milk for 30 min at room temperature, the sections were incubated overnight with rabbit anti-active-type caspase3 (BD Pharmingen, San Diego, CA, 1:50), rat anti-PECAM (BD Pharmingen, 1:500), or rabbit anti-β-galactosidase antibody at 4°C. The immunoreaction was detected using fluorophore conjugated secondary antibodies (Invitrogen). Nuclei were counterstained with 4′,6-diamidino-2-phenylindole (DAPI) (Sigma Chemical Co., St. Louis, MO). For double immunohistochemistry with rat anti-PECAM and

rabbit anti-β-galactosidase antibodies, the two antibodies were serially applied to immunohistochemical reaction.

Generation of Fkhl18-lacZ Transgenic (Tg) Mice

Cosmid genomic clones containing mouse *Fkhl18* gene were obtained from a cosmid library constructed with SuperCos-1 cosmid vector (Stratagene, La Jolla, CA) carrying hsp68-lacZ cassette (Fig. 2A). This cosmid vector was constructed to examine the enhancer activity of inserted DNAs (Zubair et al., 2006). Genomic DNAs containing 3′ regions of *Fkhl18* prepared from cosmid clone were ligated with hsp68-lacZ (Zubair et al., 2006) cassette to construct plasmids for Tg mice (Fig. 2A). The cosmid and plasmid DNAs were digested with *Not*I and *Not*I/*Sal*I, respectively, and the linear DNA fragments were used for microinjection. Tg mice were generated as described previously (Nagy et al., 2003). The DNAs of the founder animals were subjected to PCR with primers for lacZ (5′-GCC GAA ATC CCG AAT CTC TAT C-3′ and 5′-GAT TCA TTC CCC AGC GAC CAG-3′). LacZ activities of the fetuses were examined as described previously (Nagy et al., 2003).

Generation of Fkhl18 KO Mice

Fkhl18 gene is comprised by a single exon. Bacteriophage clones containing *Fkhl18* gene were obtained from 129/SvEv genomic library (Stratagene). To disrupt *Fkhl18* gene, a *Nco*I/*Kpn*I fragment of *Fkhl18* gene was substituted by IRES-lacZ-pMC1-Neo cassette (Katoh-Fukui et al., 1998; Kitamura et al., 2002). The 5′ region from the *Not*I site (0.9 kb) and 3′ region from the *Kpn*I site (6.7 kb) were used for homologous recombination (Fig. 3). The targeting linearized vector was subjected to electroporation into E14TG2a (129Ola) ES cell line (Kitamura et al., 2002). The chimeric male mice produced with the homologous recombinant ES clones were crossed with C57BL/6Jjcl females (Japan Clea). *Fkhl18* deficient heterozygous male mice obtained were backcrossed onto C57BL/6Jjcl genetic background. Three to seven generations of the mice were used to obtain homozygous *Fkhl18* KO mice. Littermates were genotyped by PCR with the following primers; Fkh3-110FW (5′-CCT CCT GAC AAA CTT GGG ATG T-3′), Fkh3-109RV (5′- TTG TGG AGG AGA CTA AGC CAC CT-3′), and OIMR014 (5′-AGG TGA GAT GAC AGG AGA TC-3′) (Fig. 3).

All animal experiments were carried out in accordance with National Institute of Health Guide for the Care and Use of Laboratory Animals and approved by the Animal Care and Use Committee of National Institute for Basic Biology.

Electron Microscopy

Wild-type (WT) and *Fkhl18* KO testes were excised from fetuses and immersed in 3% glutaraldehyde in 10 mM HEPES (*N*-2-hydroxylpiperazine-*N*′-2-ethanesulfonic acid)–NaOH (pH 7.4) and 145 mM NaCl for at least 2 hr. After fixation with 1% osmium tetroxide for 1 hr, the tissues were dehydrated and embedded in epoxy resin. Ultrathin sections were prepared, stained with uranyl acetate and lead citrate, and thereafter subjected to electron microscopic observation. Electron micrographs were taken with a JEM 1200EX electron microscope (JOEL, Tokyo, Japan) as described previously (Katoh-Fukui et al., 2005).

Visualizing Fetal Vasculature System by Ink Injection

Ink was injected as described previously (Nagy et al., 2003). E14.5 fetuses were dissected from a pregnant female with an intact yolk sac and attached placenta. The fetuses were placed in PBS at 37°C under a dissecting scope, to be kept circulation active. The tip of a glass pipette was inserted into the umbilical vessel, and carbon ink (CE 100-6, Kuretake Co., Nara, Japan) was instilled into the vessel with minute puffs of breath. The diameter of the carbon particle is longer than 50 nm (average, 180 nm). After distribution of the ink in whole body, the fetus was fixed with 4% PFA. The gonads were harvested and examined under a light microscope. To analyze the testicular distribution of the injected ink, the fetuses were cryosectioned into 10-μm thick sections.

Reporter Gene Assay and Immunocytochemistry

Full-length *Fkhl18* coding region was subcloned into pcDNA3 expression vector (Invitrogen). p6 × DBE-luc reporter plasmid carrying six repeats of Fox binding sequence, and expression vectors for FoxO3 and FoxO4 (Furuyama et al., 2000) were kindly provided by Dr. T. Furuyama (Sonoda Women's University). Human and mouse Fas ligand (*FasL*) gene promoter regions were prepared by PCR with genomic DNAs of HEK293 and Y1 cells, respectively. PCR (94°C for 15 sec, 60°C for 30 sec, 68°C for 1 min 30 sec, 30 cycles) was performed using the following primers for human *FasL* promoter, KpnI-hFasL-1500 s (5′-ATG GTA CCC CAT GTA TTT CAT CTG GCA ACC ATA AC-3′) and hFasL-1-HindIII as (5′-GCA AGC TTG GCA GCT GGT GAG TCA GGC CAG CC-3′), and for mouse *FasL* promoter, KpnI-mFasL-1534 s (5′-ATG GTA CCG TGA TTG GTG GAC AGT AGG GTG TTG-3′) and mFasL-1-HindIII as (5′-GCA AGC TTG GCA CCC AGC CCC AGG AAA GGG TTT C-3′). Approximately 1.5 kb PCR products were subcloned into pGL3-basic (Promega, Madison, WI). Human osteosarcoma U2OS cells and primary cultures of bovine aortic smooth muscle cells (Aoyama et al., 2000) were grown in Dullbecco's modified Eagle's medium (DMEM; Sigma) supplemented with 10% fetal bovine serum and 1× penicillin–streptomycin–glutamine (Invitrogen) at 5% CO_2 and 37°C. Transfection was performed as described previously (Mukai et al., 2002). pCMV-SPORT-β-gal (Invitrogen) was used as an internal control to normalize transfection efficiency. The cells were harvested 48 hr after transfection, and the cell lysates were subjected to luciferase and β-galactosidase assays as described previously (Mukai et al., 2002). All transfection experiments were performed in triplicate. Values are presented as mean ± standard deviation (SD) of three independent experiments.

For immunocytochemistry, U2OS cells were seeded on coverslips and then subjected to transfection as described above. The cells were fixed 48 hr after transfection in 4% PFA, blocked with 1.5% skim milk, and then incubated with anti-myc (N-14, Santa Cruz Biotechnology, Santa Cruz, CA) and anti-HA (12CA5) antibodies. For fluorescent detection, Alexa Fluor 488 anti-rabbit antibody (Invitrogen) and Cy3 anti-mouse antibody (Invitrogen) were used, respectively. Nuclei were counterstained with DAPI (Sigma).

Electrophoretic Mobility Shift Assay (EMSA)

Double-stranded oligonucleotides containing 5′ protruding ends were labeled with ^{32}P-dCTP and Klenow polymerase. The nucleotide sequences for the probes were 5′-GATCAAGTAAACAACTATGT-3′/5′-CTAGACATAGTTGTTTACTT-3′ for WT probe and 5′-GATCAAGTAAGCAACTATGT-3′/5′-CTAGACATAGTTGCTTACTT-3′ for mutated probe (underlined nucleotide are mutated). Fkhl18-myc was prepared using a coupled TNT transcription and translated kit (Promega). EMSA was performed as described previously (Morohashi et al., 1992).

RESULTS

Expression of Fkhl18 in Periendothelial and Sertoli Cells of Fetal Testis

To examine the tissue specificity of *Fkhl18* expression during mouse fetal development, RT-PCR was performed with RNAs prepared from various tissues at E16.5 (Fig. 1A). Although the expression of *Fkhl18* was detected in many tissues examined, the expression in the testis was clearly higher than others including the ovary. Next, we determined the type of fetal testicular cells that expressed *Fkhl18* by in situ hybridization. The in situ signals were detected both inside and outside (interstitial region) of the testis cord (Fig. 1B-a). Immunohistochemical staining with anti-Ad4BP/SF-1 after the in situ analysis showed that Ad4BP/SF-1 immunoreactive nuclei are surrounded by in situ signals in the testicular cord (Fig. 1B-b, arrows), strongly suggesting that *Fkhl18* is expressed in Sertoli cells.

The interstitial region of the developing fetal testis is occupied by different cell types, such as fetal Leydig cells, peritubular cells, periendothelial cells (pericytes), endothelial cells, and uncharacterized fibroblast-like cells. Moreover, a large coelomic vessel is characteristic for the fetal testis. Vascular blood vessels are generally composed of endothelial cells and vascular smooth muscle cells, which encircle endothelial cells to act as a supporting structure of the vessel. However, at the early stage of blood vessel formation, vascular smooth muscle cells are still immature and thus referred as periendothelial cells. To identify the cells that express *Fkhl18*, we localized PECAM1-positive endothelial cells in sections next to those used for in situ hybridization for *Fkhl18*. As shown in Figure 1B, the PECAM1-positive endothelial cells of the coelomic vessel (Fig. 1B-c) and inner testicular vessel (Fig. 1B-e) seemed to be encircled by

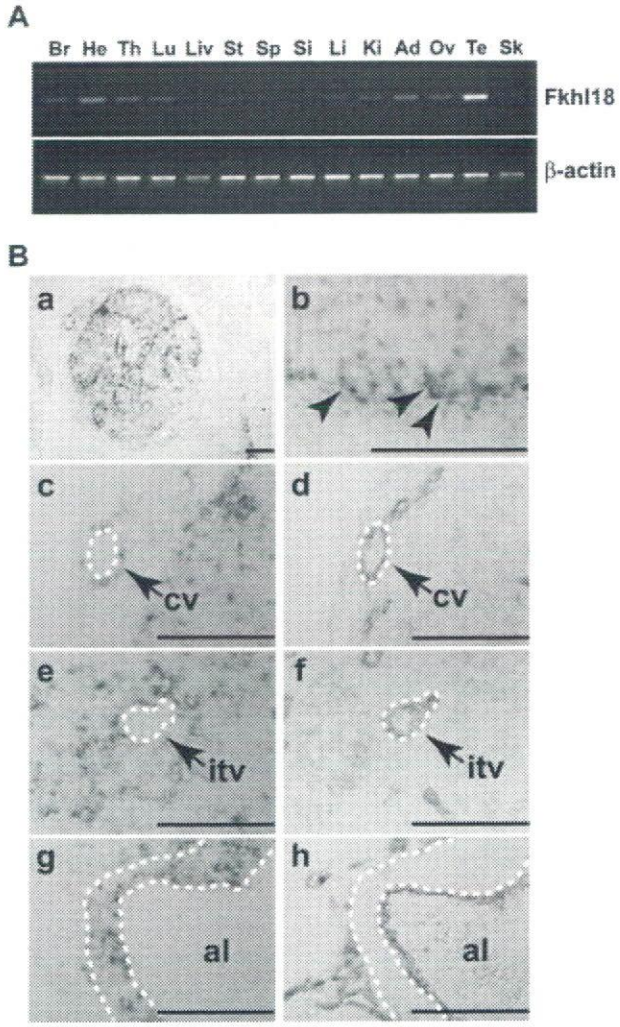

Fig. 1. Expression of Fkhl18 in the developing tissues of mouse fetuses. **A**: Analyses of *Fkhl18* gene expression by RT-PCR. Total RNAs prepared from E16.5 fetal tissues were subjected to RT-PCR with sets of primer for *Fkhl18* and β-actin. Br; brain, He; heart, Th; thymus, Lu; lung, Liv; liver, St; stomach, Sp; spleen, Si; small intestine, Li; large intestine, Ki; kidney, Ad; adrenal gland, Ov; ovary, Te; testis, Sk; skin. **B**: Expression of *Fkhl18* in E14.5 male gonad. In situ hybridization probed with *Fkhl18* was performed with E14.5 male gonad (a, b, c, e). The section used for in situ hybridization was further subjected to immunohistochemistry with antibody for Ad4BP/SF-1 (b). As indicated by arrowheads in (b), Sertoli cells in the testis cord are double positive for *Fkhl18* and Ad4BP/SF-1. Cells surrounding the coelomic vessel (cv; indicated by dotted line in c) and inner testis vessel (itv; indicated by dotted line in e) provided the in situ signals. *Fkhl18* in situ signal surrounding an aorta (g) is shown (g). al; aortic lumen. Sections next to (c), (e), and (g) were subjected to immunostaining with antibody to PECAM1 in (d), (f), and (h), respectively. Scale bars = 100 μm.

Fkhl18-expressing cells (Fig. 1B-d,f). Likewise, examination of the aorta showed a similar correlation of expressions between *Fkhl18* and PECAM1 (Fig. 1B-g,h). These expression profiles of *Fkhl18* and PECAM1 suggest that *Fkhl18* is expressed in periendothelial cells. To confirm this, we tried to perform double staining for *Fkhl18* in situ and PECAM1 immunohistochemistry. Unfortunately, however, immunohistochemistry with PECAM1 did not work after the

reaction of in situ hybridization. Moreover, we attempted to prepare antisera for *Fkhl18*, but could not obtain any antisera applicable for immunohistochemical study.

Instead, we generated transgenic (Tg) mice with *lacZ* reporter gene to recapitulate the endogenous expression of *Fkhl18*. Cosmid clones, cF6 and cF8 (Fig. 2A), carrying whole genomic regions of intron-less *Fkhl18* were obtained by screening of a mouse cosmid library. Since the cosmid vector used for library preparation carries Hsp68-*lacZ* cassette, transcriptional enhancer activity of the inserted DNA is evaluated by lacZ staining (Zubair et al., 2006). The Tg mouse fetuses harboring cF6 and cF8 successfully induced *lacZ* expression in both the gonad and blood vessels (Fig. 2B). The region overlapped by the two cosmid DNAs was fragmented and used for preparation of transgenes with the Hsp68-*lacZ* cassette. The recombinant plasmid DNAs, #43, #51, and #60, were subjected to Tg assays. As summarized in Figure 2B, plasmid #51 could induce *lacZ* expression in the fetal gonad of both sexes and blood vessels (Fig. 2C) similar to the original cosmid clones, cF8 and cF6, whereas plasmids #43 and #60 induced *lacZ* expression in blood vessels and gonads, respectively. Thus, the testes of Tg fetuses carrying plasmid #51 were examined immunohistochemically with antibodies to lacZ and PECAM1 to determine which cells express *Fkhl18*. As shown in Figure 2D, the endothelial cells of the coelomic vessels are immunoreactive for PECAM1 (green), and PECAM1-positive endothelial cells are obviously lined by lacZ (red)-positive cells. Considering that the two stainings are not overlaid mutually, *Fkhl18* is obviously expressed in periendothelial cells.

Abnormal Testicular Vasculature in Fkhl18 Deficient Mice

To investigate the function of *Fkhl18*, we generated a gene disrupted mouse. The *Nco*I/*Kpn*I fragment of the *Fkhl18* gene encoding from 29th to 329th amino acid residues was replaced by IRES-lacZ-pMC1neo cassette (Fig. 3A). *Fkhl18* disrupted allele was confirmed by Southern blotting (Fig. 3B,C) and PCR (Fig. 3D). The resultant heterozygous crosses yielded homozygous, heterozygous, and WT individuals at Mendelian ratios when examined at fetal life and adulthood (data not shown). Expectedly, *Fkhl18* mRNA was depleted from the *Fkhl18* KO testes (Fig. 3E). Although the reason was not clear, we could not detect any lacZ signals in the heterozygous and KO fetuses.

The homozygous *Fkhl18* KO male and female mice were healthy and fertile. Being consistent with unaffected fertility, Sertoli cells in the KO testes were apparently normal. However, we noticed accumulation of blood in the central part of the testes in *Fkhl18* KO mice (Fig. 4A). The incidence of this abnormal feature was 33% in homozygous KO but 0% in the WT, when examined in the testes of 14 WT, 26 heterozygous, and 12 homozygous KO (Fig. 4B). Interestingly, this phenotype was observed even in the heterozygous testes and the frequency seemed to correlate with the dosage of the gene.

To visualize the entire structure of the testicular vasculature system, we injected carbon ink into the umbilical vein of E14.5 fetuses. Although the whole view of branches of the vasculature system was indistinguishable between the WT and *Fkhl18* KO testes (Fig. 4C-a,b), the area around the vasculature looked

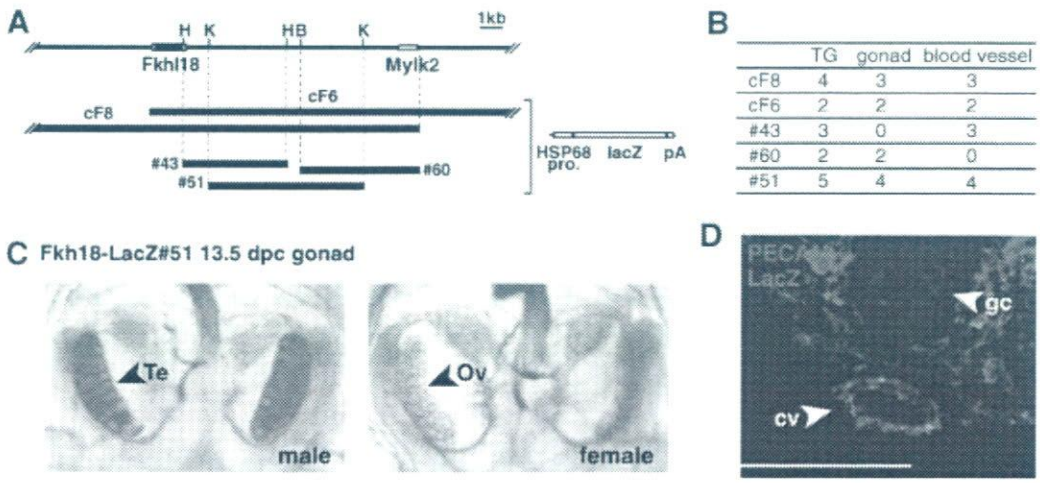

	TG	gonad	blood vessel
cF8	4	3	3
cF6	2	2	2
#43	3	0	3
#60	2	2	0
#51	5	4	4

Fig. 2. Expression of Fkhl18 in the periendothelial cells of mouse fetal testis. **A**: DNA construction for Tg mouse assay. Cosmid clones, cF6 and cF8, were isolated from a library prepared with cosmid vector carrying hsp68-lacZ cassette. A region overlapped by these two cosmid clones was fragmented and ligated to hsp68-lacZ cassette to produce plasmid clones, #43, #51, and #60. H; *Hin*dIII, K; *Kpn*I, B; *BamH*I. **B**: Summary of Tg assays with the recombinant Tg constructs. The cosmid (cF6 and cF8) and plasmid (#43, #51, and #60) recombinant DNAs were used to generate Tg mice, and lacZ expression in the fetal gonad and blood vessel was examined at E13.5. Numbers represent those of Tg fetuses examined, and those displaying lacZ activity in the gonad and blood vessels. **C**: LacZ expression in Tg mice. Tg mice were produced with the #51 recombinant DNA. Representative expression patterns of *lacZ* are shown in male (left) and female (right) fetuses at E13.5. Te; testis, Ov; ovary. **D**: Expression of *LacZ* in periendothelial cells. The testis of the Tg fetus (#51) at E14.5 was subjected to immunohistochemical analyses with antibodies to PECAM1 (green) and lacZ (red). Note the signals for PECAM1 in endothelial cells of coelomic vessel (cv) and germ cells (gc). Note also signal for lacZ in periendothelial cells.